

A catalogue of Large Magellanic Cloud star clusters observed in the Washington photometric system

T. Palma^{1,2,3}, L.V. Gramajo³, J.J. Clariá^{3,4}, M. Lares^{3,4,5}, D. Geisler⁶, and A.V. Ahumada^{3,4}

¹ Millennium Institute of Astrophysics, Nuncio Monseñor Sotero Sanz 100, Providencia, Santiago, Chile

² Instituto de Astrofísica, Pontificia Universidad Católica de Chile, Av. Vicuña Mackenna 4860, 782-0436 Macul, Santiago, Chile
e-mail: tpalma@astro.puc.cl

³ Observatorio Astronómico, Universidad Nacional de Córdoba, Laprida 854, 5000 Córdoba, Argentina

⁴ Consejo Nacional de Investigaciones Científicas y Técnicas (CONICET), Argentina

⁵ Instituto de Astronomía Teórica y Experimental (IATE), Laprida 922, Córdoba, Argentina

⁶ Departamento de Astronomía, Universidad de Concepción, Casilla 160-C, Concepción, Chile

Received ; accepted

ABSTRACT

Aims. The main goal of this study is to compile a catalogue including the fundamental parameters of a complete sample of 277 star clusters (SCs) of the Large Magellanic Cloud (LMC) observed in the Washington photometric system, including 82 clusters very recently studied by us.

Methods. All the clusters' parameters such as radii, deprojected distances, reddenings, ages and metallicities have been obtained by applying essentially the same procedures which are briefly described here. We have used empirical cumulative distribution functions to examine age, metallicity and deprojected distance distributions for different cluster subsamples of the catalogue.

Results. Our new sample made up of 82 additional clusters recently studied by us represents about a 40% increase in the total number of LMC SCs observed up to now in the Washington photometric system. In particular, we report here the fundamental parameters obtained for the first time for 42 of these clusters. We found that single LMC SCs are typically older than multiple SCs. Both single and multiple SCs exhibit asymmetrical distributions in log (age). We compared cluster ages derived through isochrone fittings obtained using different models of the Padova group. Although t_G and t_B ages obtained using isochrones from Girardi et al. (2002) and Bressan et al. (2012), respectively, are consistent in general terms, we found that t_B values are not only typically larger than t_G ages but also that Bressan et al.'s age uncertainties are clearly smaller than the corresponding Girardi et al. values.

Key words. techniques: photometric – galaxies: individual: LMC – galaxies: star clusters: general

1. Introduction

The Magellanic Clouds have long been considered an ideal laboratory to study a variety of objects and phenomena in nearby galaxies. In particular, the Large Magellanic Cloud (LMC) has been a target of intensive research because of its proximity and its almost face-on position in the sky (Harris & Zaritsky 2009), which facilitates a detailed analysis of its stellar populations. Various studies of LMC star clusters (SCs) have shown that these stellar populations differ from Galactic SCs in their typical radii, masses, kinematics, age distribution, etc. The nature and cause of the so called cluster age-gap of approximately 3 to about 12 Gyr, with only a single cluster lying in this range in the LMC (Geisler et al. 1997) still remains of great interest, even more so if it is taken into account that a variety of HST observations have revealed that the corresponding age-gap in the field stars does not exist (e.g., Holtzman et al. 1999; Smecker-Hane et al. 2002). Unfortunately, this vast cluster age-gap does not allow us to use SCs to trace the chemical enrichment and star-formation history of the LMC during such a long period of quiescence. However, the great abundance of clusters outside of this gap make them excellent tracers of these quantities otherwise.

The Washington photometric system, originally defined to study G and K late-type stars and old stellar populations

(Canterna 1976) and later calibrated by Geisler et al. (1991), has been widely applied to young, intermediate-age and old clusters in the Galaxy (e.g., Clariá et al. 2007; Piatti et al. 2009a) and in the Magellanic Clouds (e.g. Geisler et al. 2003). This system has proved to be an excellent tool to determine a variety of astrophysical parameters such as distances, interstellar absorption, ages and particularly chemical abundances (metallicities) for SCs as well as for field stars located in the cluster surrounding regions. The advantages that this system offers to study Galactic and/or extragalactic SCs have been demonstrated by Geisler et al. (1991, 1997) and Geisler & Sarajedini (1999). In particular, the combination of the Washington system C and T_1 filters is approximately three times more metallicity-sensitive than the corresponding VI standard giant branch technique. This, combined with the Washington system's broad and efficient passbands, makes it a very powerful tool for exploring stellar populations in both nearby and especially more distant galaxies. In addition, Geisler (1987) has shown that the system can be made even more efficient by substituting the Kron-Cousins R filter for the standard Washington T_1 filter. In fact, the R filter has a very similar wavelength coverage but a significantly higher throughput as compared to the standard Washington T_1 filter. Therefore, R instrumental magnitudes can be easily and accurately transformed to yield standard T_1 magnitudes. As shown by Geisler & Sarajedini (1999), the combined use of the

C and R filters allows us to derive accurate metallicities based on their standard giant branch (SGB) technique. Using LMC SCs observed in the Washington photometric system, we have recently examined the chemical enrichment history of the LMC during the last 2-3 Gyr (Palma et al. 2015).

The fundamental parameters of a total of 195 LMC SCs have been determined using the Washington system in a number of papers over the years. A short description of the selected sample criteria is summarized in Table 1. We have recently published the results obtained for 40 unstudied or poorly studied SCs (Palma et al. 2013, 2015). In the current study, we report the results obtained for another 42 LMC SCs, all of them observed in the Washington system. Thus, this combined sample of 82 clusters represents about a 40% increase in the total of LMC clusters observed and studied up to this moment in the Washington photometric system. Since all the clusters' parameters were obtained by applying essentially the same procedures, this group of objects represents a uniform and homogeneous cluster sample. Although the total sample still represents only a tiny fraction of the very populous LMC SC system, it is in fact one of the largest and most uniform LMC SC samples available and thus a catalogue uniting the combined information in a single dataset should be of substantial general astrophysical use.

2. Observations

We have compiled a catalogue including a total of 277 LMC SCs studied in the Washington system. All the photometric observations of these SCs were carried out at Cerro Tololo Inter-American Observatory (CTIO, Chile), using the Washington C and T_1 filters (Canterna 1976) and the Kron-Cousins R filter. As mentioned in Palma et al. (2015), our new sample of 82 SCs was observed with the CTIO “V́ctor Blanco” 4 m telescope in December 2000. The CTIO 0.9 m telescope was used by Geisler et al. (1997, 2003), Bica et al. (1998) and Piatti et al. (2002, 2003a,b, 2009b, 2011), while the observations reported by Geisler (1987), Piatti (2011, 2012); Palma et al. (2013, 2015) and Choudhury et al. (2015) were also carried out with the CTIO 4 m telescope. Only one LMC cluster (NGC 2213) was observed with the CTIO 1.5 m telescope. The seeing at CTIO was typically 1-1.5 arcsec during all the observing nights.

The total cluster sample is presented in Table 2, where we list the various star cluster designations from different catalogues, 2000.0 equatorial coordinates, Galactic coordinates, and the cluster core radii given by Bica et al. (2008). These core radii constitute half of the mean apparent central diameters obtained by computing the average between the major (a) and minor (b) axes. Figure 1 shows a distribution map of the whole sample of LMC clusters studied in the Washington photometric system superimposed on the LMC image. The dashed lines delimit the LMC bar region. Filled circles represent the 82 clusters of our recent sample, while plus signs stand for clusters studied by other authors using the same technique and analysis procedures.

3. Fundamental parameters

The procedures applied by both ourselves as well as other authors to determine the LMC SCs fundamental parameters in

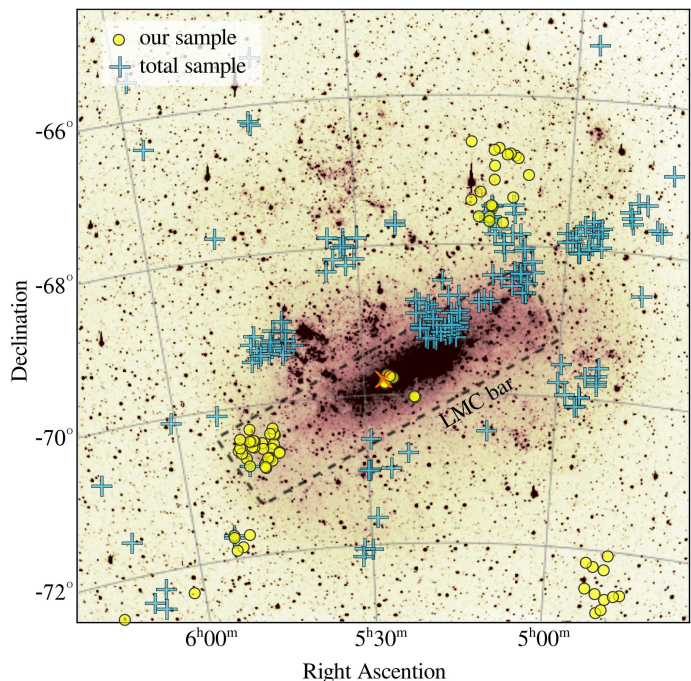


Fig. 1: Distribution map of the whole sample of star clusters studied in the Washington photometric system superimposed on the LMC galaxy image. Filled circles represent the 82 clusters of our own sample, while plus signs stand for clusters studied by other authors using the same technique and analysis procedures. The cross indicates the geometrical centre of the bar (Bok 1966). The credits for the background image belongs to Bothun & Thompson (1988), Kennicutt et al. (1995) and Parker et al. (1998).

the Washington system are briefly described below. For further details see Palma et al. (2013) and references therein.

Cluster radii: the procedure generally applied to determine a cluster's radius is based on obtaining the radial profile of the stellar density surrounding the cluster. Firstly, it is necessary to determine the cluster centre through Gaussian distribution fits to the star counts performed in the x and y directions. The most important sources of uncertainty in the placement of cluster centres come from the relatively small ratio between the number of cluster and field stars, and the projected intracluster fluctuations due to both cluster and field star density variations. Then, the cluster radial profile is built by computing the number of stars per unit area at a given radius r . Once the level of the background is estimated beyond the observed cluster boundary, the radius of the cluster is defined as the distance from the cluster's centre where the number of stars per unit area (cluster+background) equals that of the estimated background level. Error estimates for the radii range typically between 0.05' and 0.2', according to the telescope used, the concentration of the cluster and the position within the LMC. Examples of the procedure here described to determine clusters' radii can be seen in Palma et al. (2013). In a few cases, when the clusters appear to be too faint if compared to the “noisy” background, the core radii reported by Bica et al. (2008) were adopted.

Angular deprojected distances: the angular deprojected distance of a LMC cluster is the distance, measured in degrees, from the optical centre of the LMC to the cluster, taking into ac-

Table 1: Description of selected LMC SC samples found in the literature

Authors	Selected SCs	Characteristics / selection criteria	CTIO Telescope
Geisler (1987)	1	Technique tests	1.5m
Geisler et al. (1997)	25	Search for old SC candidates	0.9m
Bica et al. (1998)	13	SC properties in the outer LMC	0.9m
Piatti et al. (2002)	2	Cluster age gap and first metallicity determination	0.9m
Geisler et al. (2003)	8	Metallicity determinations for some SCs from Geisler et al. (1997)	0.9m
Piatti et al. (2003b)	11	Blue SCs in the west region of the LMC bar	0.9m
Piatti et al. (2003a)	6	Systematic study	0.9m
Piatti et al. (2009b)	5	Systematic study; mostly unstudied clusters	0.9m
Piatti (2011)	36	Bursting forming episode	4m
Palma et al. (2011)	4	Systematic study; unstudied clusters	4m
Piatti (2012)	26	Enlarging the sample of SCs in the 100-1000 Myr age range	4m
Palma et al. (2013)	23	Systematic study; mostly unstudied clusters; age/metallicity gradients	4m
Piatti (2014)	90	Search for genuine SCs and age determinations	4m
Palma et al. (2015)	17	Systematic study; mostly unstudied clusters; age-metallicity relation	4m
Choudhury et al. (2015)	45	Search for genuine SCs and characterization	4m

count the depth of the LMC and is computed using the following expression (Clariá et al. 2005):

$$d = d(p)\{1 + [\sin(p - p')^2][tg(i)^2]\}^{0.5}, \quad (1)$$

where d is the cluster angular deprojected distance, $d(p)$ the angular projected distance on the plane of the sky, p the position angle of the cluster (measured in the usual sense towards E starting from N), p' the position angle of the line of nodes and i the tilt of the LMC plane to the plane of the sky. The position of the cluster NGC 1928 (J2000, $\alpha = 5^h20^m47^s$ $\delta = -69^\circ28'41''$) was adopted as the LMC optical centre. To compute d from equation (1), we adopted $i = 35.8^\circ \pm 2.4^\circ$ and $p' = 145^\circ \pm 4^\circ$ for the tilt of the LMC plane and the position angle of the line of nodes, respectively (Olsen & Salyk 2002). We carried out an error analysis in order to measure the uncertainties involved in the geometric parameters. We found that our estimated error in deriving this quantity increases with the angular projected distance reaching a maximum value of $\sim 0.3^\circ$.

Interstellar reddening and cluster distances: cluster-reddening values have usually been estimated by interpolating the extinction maps of Burstein & Heiles (1982). These maps were obtained from HI (21 cm) emission data for the southern sky and provided us with foreground $E(B - V)$ colour excesses, which depend on the Galactic coordinates. As shown in Col. 4 of Table 2, the resulting $E(B - V)$ values for the whole cluster sample range between 0.00 and 0.23, which are typical values for the LMC. As explained in previous studies, we preferred not to use the full-sky maps from 100- μ dust emission obtained by Schlegel et al. (1998) since the dust temperature and reddening derived from pointing towards the LMC and other bright extragalactic sources are not reliable in these cases (e.g. Piatti et al. 2011). As for the cluster distance moduli, the value of the LMC true distance modulus $(m - M)_0 = 18.50 \pm 0.10$ reported by Saha et al. (2010) has always been adopted. According to Subramanian & Subramaniam (2009), the average depth for the LMC disc is 3.44 ± 0.16 kpc. Keeping in mind that any LMC cluster could be situated in front of or behind the main body of the LMC, we come to the conclusion that the difference in apparent distance modulus could be as large as $\Delta(V - M_V) \sim 0.3$ mag. Given that the average uncertainty when adjusting the isochrones to the cluster colour-magnitude diagrams (CMDs) is 0.2-0.3 mag, adopting one single value for the distance modulus

of all the clusters should not dominate the error budget in the final results.

Ages and metallicities: cluster ages and metallicities have been usually determined by applying two different and independent procedures. In both cases, however, it is necessary to first obtain the observed cluster ($C - T_1, T_1$) CMD and then to minimize the field star contamination in this diagram. The CMDs of the 82 clusters of our recent sample were cleaned by using a statistical method developed by Piatti & Bica (2012). Once the cleaned CMDs of the clusters are obtained, the first method consists in selecting a set of theoretical isochrones corresponding to different ages and metallicities and superimposing them on the cleaned cluster CMDs, once they were properly shifted by the corresponding $E(B - V)$ colour excess and LMC distance modulus. The age and metallicity adopted for each cluster are those corresponding to the isochrone which best matches the shape and position of the cluster main sequence (MS), particularly at the turn-off (TO) level, as well as the T_1 magnitude of the red giant clump (RGC). To apply this method, theoretical isochrones computed for the Washington system by the Padova group (Girardi et al. 2002; Bressan et al. 2012) and Geneva group (Lejeune & Schaerer 2001) have been used. Lejeune & Schaerer (2001) and Girardi et al. (2002) isochrones have been computed for chemical compositions of $Z = 0.019, 0.008$ and 0.004 , equivalent to $[\text{Fe}/\text{H}] = 0.0, -0.4$ and -0.7 , while Bressan et al. (2012) more recent models include isochrones having metallicities between $[\text{Fe}/\text{H}] = -0.19$ and -0.84 , which vary in an almost continuous way. Although for 23 out of the 82 clusters of our sample reported in Palma et al. (2013) we initially used Girardi et al. (2002) isochrones, for the present analysis we have used Bressan et al. (2012) isochrones for the entire sample because the latter include much smaller intervals in chemical composition (Z) than those used by Girardi et al. (2002). Thus, more precise fits could then be obtained. In general, the different sets of theoretical isochrones both from Padova and Geneva lead to nearly similar results. The differences arising when different sets of isochrones of the Padova group are used can be seen in Figure 5.

A second method to derive cluster ages is based on the δT_1 parameter, defined as the difference in T_1 magnitude between the RGC and the MSTO in the Washington ($C - T_1, T_1$) CMD.

The age is obtained from the following equation given in Geisler et al. (1997):

$$\text{Age}(\text{Gyr}) = 0.23 + 2.31 \times \delta T_1 - 1.80 \times \delta T_1^2 + 0.645 \times \delta T_1^3, \quad (2)$$

with a typical error of ± 0.3 Gyr. Age determination via δT_1 , however, is applicable only to intermediate-age (IACs) and/or old clusters, i.e., generally older than 1 Gyr. Even though some clusters appeared to be IACs (1-3 Gyr), it was not possible to determine their ages from δT_1 due to the fact the RGC in their CMDs was not clearly visible. This happened because sometimes the central regions of the clusters seem to be saturated, or there are just very few RC stars in some faint clusters, or else they are not photometrically well resolved in the images. In these cases, the RG stars are missing or poorly defined and therefore no clump can be clearly detected in the CMDs. The resulting δT_1 values and the corresponding cluster ages are listed in Col. 7 of Table 3.

Metallicities have also been obtained utilizing the SGBs of Geisler & Sarajedini (1999) by placing the observations in the $[M_{T_1}, (C - T_1)_0]$ plane utilizing the equations $E(C - T_1) = 1.97E(B - V)$ and $M_{T_1} = T_1 + 0.58E(B - V) - (V - M_V)$. Each SGB corresponds to an iso-abundance curve. As these authors pose, however, this procedure can be applied only to SCs aged 2 Gyr or older. Geisler & Sarajedini (1999) demonstrated that the metallicity sensitivity of the SGBs is three times higher than that of the V, I technique (Da Costa & Armandroff 1990). Consequently, it is feasible to determine metallicities three times more precisely for a given photometric error. The SGB method consists of inserting absolute M_{T_1} magnitudes and intrinsic $(C - T_1)_0$ colours for the clusters into Fig. 4 of Geisler & Sarajedini (1999) to roughly derive their metal abundances ($[\text{Fe}/\text{H}]$) by interpolation. The metallicities derived through this method were corrected for age effects for younger clusters, following the recommendations made by Geisler et al. (2003). The resulting age corrected metallicities are shown in Col. 8 of Table 3, with typical errors of 0.3 dex.

4. Catalogue description

We have compiled a catalogue in which we included the fundamental parameters of 277 LMC SCs observed in the Washington photometric system. All these clusters have been studied and analyzed in a homogeneous way. The same procedures have been applied not only by our team but also by the other studies used in this compilation. The catalogue presented in Table 3 is structured as follows:

- ID: cluster designations from different catalogues.
- Cluster radius: distance r in arcminutes from the cluster's centre up to the region where the stellar density equals that of the background.
- Angular deprojected distance: distance, measured in degrees, from the LMC optical centre to the cluster.
- $E(B-V)$: cluster reddening.
- Age_I : age in gigayears determined from isochrone fittings.
- $[\text{Fe}/\text{H}]_I$: metallicity determined from isochrone fittings.
- Age_H : age in gigayears derived from the δT_1 method.
- $[\text{Fe}/\text{H}]_H$: metallicity estimated from the SGB procedure of Geisler & Sarajedini (1999).

- Notes: letters a, b and c indicate that the clusters have also been studied in other photometric systems. Letter m denotes that the cluster is part of a binary or a multiple system (Dieball et al. 2002).
- Ref: references to the works from which we took the fundamental parameters determined by other authors in the Washington photometric system.

5. Statistical analysis

5.1. The empirical cumulative distribution function (ECDF)

Although the age and metallicity distributions of the LMC SCs can be examined and compared by computing their respective histograms, the corresponding empirical cumulative distribution functions (ECDFs) are preferred since they are independent of the particular selection of the binning function employed to build the histograms. The ECDF of a random sample of observations x_1, x_2, \dots, x_n is a function $F_n(t)$ given by the fraction of objects in the sample which are equal to or lower than an arbitrary value t . This function is equivalent to the original data. Its use avoids the loss of information brought about by the rounding off that results from placing the data in integer bin units when histograms are constructed (e.g. Drion 1952).

The ECDF can also be used to compare two samples and assess whether they are intrinsically different or just random realizations of the same parent distribution which appear different because of the stochastic nature of the data. The maximum difference between the two ECDFs, denoted by D , is commonly used as an indicator of the distinctiveness of the two data sets. This is the basis of the Kolmogorov-Smirnov test or KS-test (e.g. Press et al. 1992), which allows one to quantitatively contrast the hypothesis that the two samples are drawn from the same parent distribution to a given significance level, with the alternative hypothesis that the two samples are not taken from the same population. The statistic of this test has a known distribution that permits computing the p-value, i.e., the probability of obtaining, in two random samples, a value of the variable D equal to or larger than the one observed for the two particular data sets. Being nearly distribution free, this statistic is fairly easy to compute (Ross 2012).

5.2. Statistical results

We adopted the above defined ECDF to study the age and metallicity results obtained for different LMC cluster samples. The ECDF was also used to analyze the advantages of employing different sets of theoretical isochrones. Four different LMC SC samples are considered for our statistical analysis. The first of these samples, called S0, includes all the SCs whose ages and metallicities have been determined by any other procedure. A second sample (S1) includes the 82 SCs of our own recent sample. A third (S2) is made up of all 277 SCs that have been observed and studied in the Washington photometric system up to this moment, i.e. this catalogue. A fourth sample (S3) represents the difference S2-S1. Table 4 shows the designations given to the different LMC cluster samples considered.

5.2.1. Metallicity distributions

Panel (a) of Figure 2 exhibits the metallicity ($[\text{Fe}/\text{H}]_I$) histograms (number of clusters per metallicity interval) corre-

Table 4: Designations of the different samples used

Name	Description	Number of SCs
S0	Full LMC cluster sample	1970
S1	Our cluster sample	82
S2	Full Washington cluster sample	277
S3	S2-S1	195

sponding to cluster samples S2 (empty bars) and S1 (dashed bars), respectively. Although the metallicity distribution of the clusters belonging to S2 is narrower compared to that of cluster sample S1, the locations of the peaks of these two distributions are very similar within the errors ($< [Fe/H] > = -0.39$ and -0.42 for S2 and S1, respectively). In fact, a t-test for the difference of the mean metallicity values yields a result consistent with zero, to a statistical significance level of 95%. Given the statistical evidence, it is not possible to conclude that there is a significant difference between samples S1 and S2. This suggests that S1 and S2 come from the same parent distribution as far as metallicity is concerned. Also, the kurtosis is positive for the two samples (5.5 and 3.2 for S1 and S2, respectively), which indicates that although the S2 distribution is more concentrated around its mean value, both S1 and S2 are distributions narrower than what would be expected from a Gaussian distribution. More than 60% of the clusters in S2, for example, have metallicities in the $[-0.45, -0.35]$ range, in contrast with less than 30% of the clusters in S1, for the same metallicity range. This difference may be due to the fact that for most of the clusters in the S2 sample, metallicities have a fixed value of -0.4 dex. In panel (b) of the same figure, the metallicity ECDFs obtained using Girardi et al. (2002) and Bressan et al. (2012) isochrone sets are shown by dashed and solid lines, respectively. Note that Girardi et al. (2002) models only admit the adoption of discrete metallicity values (-0.7 , -0.4 and 0.0 in our case). Note as well that there is a large jump in the metallicity ECDF at $[Fe/H] = -0.4$, as this is precisely the most frequent value. On the other hand, the metallicities obtained by using Bressan et al. (2012) isochrones are distributed over different values in the same metallicity range. In this case, the metallicity ECDF is represented by a smoother curve and the metallicity mode is equal to -0.36 . The difference between this value and the above mentioned -0.4 exceeds the mean metallicity error as a consequence of the procedures used to estimate the metallicities from isochrone fittings.

5.2.2. Age distributions

The age histograms and age ECDFs for different LMC cluster samples are shown in Figure 3. In the upper panel (a), S0 and S2 samples are represented by empty bars and dashed bars, respectively. It can be clearly seen that the ages at which these two distributions reach their peak values are different. Indeed, the corresponding age of the S2 peak distribution is about 1.90 Gyr larger than that of S0. However, the shapes of these two distributions are fairly similar, since their skewness values are nearly the same. Indeed, while 67% of the clusters in S2 are younger than 1 Gyr, this percentage in the full cluster sample S0 rises to 90%. This difference may result from the differing selection of targets made for each sample. In fact, most of the clusters included in S0, for example, have been studied by Pietrzyński & Udalski (2000) and Glatt et al. (2010) who selected clusters younger than 1 Gyr. The age shift could also be partially reflecting the fact that cluster ages in S1 and S3

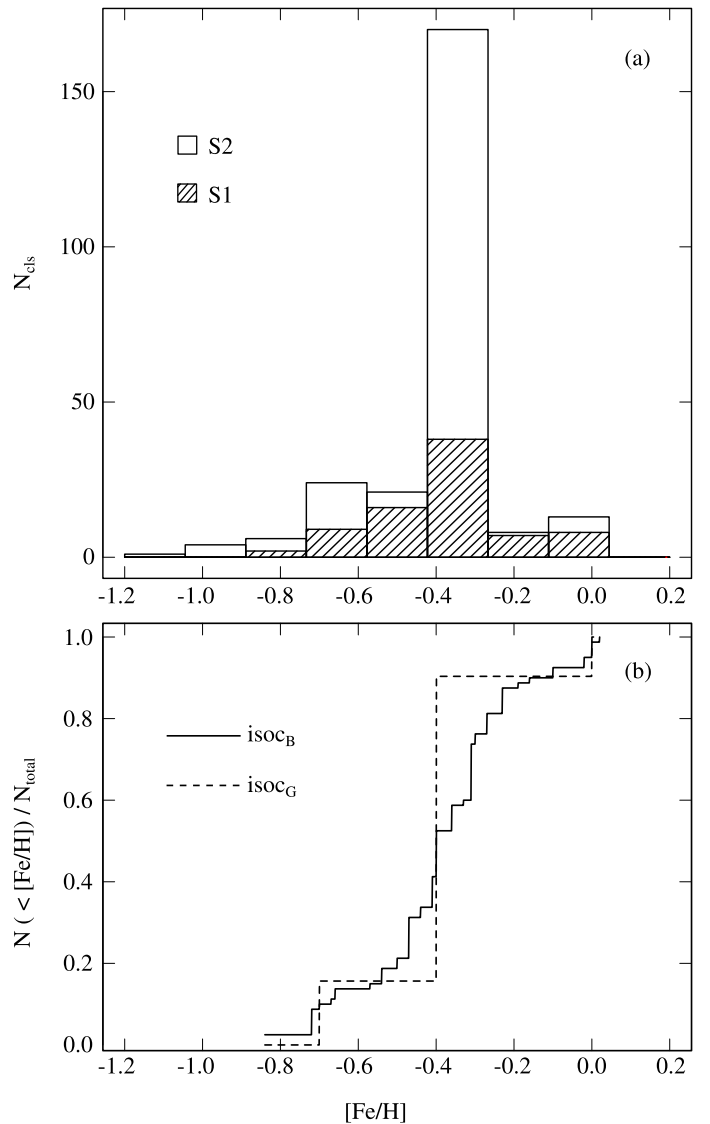


Fig. 2: Panel (a): histograms showing the metallicity distributions of LMC SCs in the S2 (empty bars) and S1 (dashed bars) cluster samples, respectively. Panel (b): comparison of metallicity ECDFs obtained for our own cluster sample S1 using sets of isochrones computed by Girardi et al. (2002, dashed line) and Bressan et al. (2012, solid line).

were estimated only from Washington photometric data, while those in S0 were obtained using different photometric systems (UBV, Washington, etc.). Age dispersions are also different, being 10% larger in S0 than in S2. To quantify this difference, we performed a test for the ratio of variances of these two distributions, thus obtaining a difference of 1 to a statistical significance level of 95%. In the lower panel (b) of Fig. 3, different age ECDFs are shown. In the inset plot, the age error distributions for S1 and S3 samples are presented. Note that the age uncertainties are clearly smaller in the S1 sample. Indeed, 80% of S1 clusters have uncertainties lower than 0.08 Gyr, while the lower tail of the uncertainties in the S3 sample reaches 0.3 Gyr. The mean values of these two distributions differ by 0.06 Gyr, which implies that the mean age uncertainty in S3 is more than twice the value of S1. A KS-test rejects the possibility that both distributions are consistent with a p-value of 0.003.

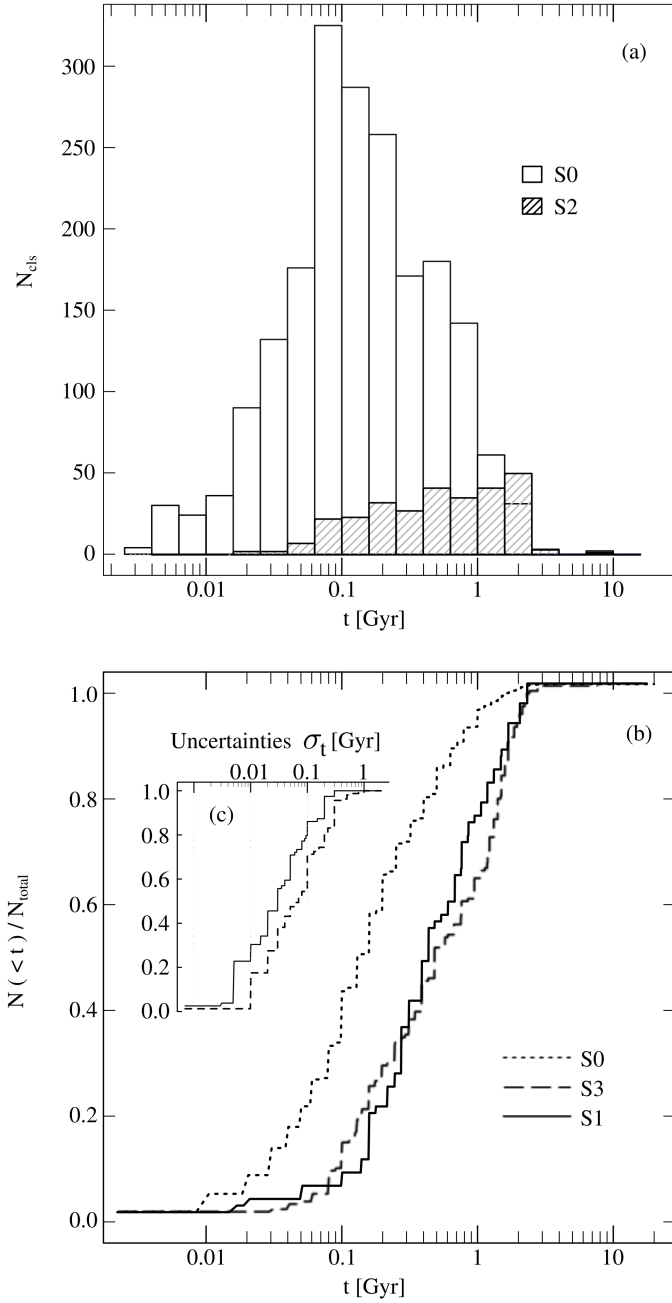


Fig. 3: Panel (a): histograms showing the age distributions obtained for the S0 (empty bars) and S2 (dashed bars) cluster samples. Panel (b): age ECDFs for S1 (solid line), its complementary sample S3 (dashed line), and S0 (short dashed line) cluster samples. The cumulative distribution estimates of age uncertainties are also shown inset in the figure.

5.2.3. Age and characteristics of single and multiple star clusters

We also examined the differences existing between the ages of single and multiple systems in the LMC. According to Dieball et al. (2002), multiple systems appear to be formed by close pairs or more clusters on the plane of the sky due to projection effects. In panel (a) of Figure 4, the ECDFs for multiple (dashed dotted line) and single SCs (dotted line) are plotted. The corresponding age histograms as well as the kernel density estimations for these two distributions are also shown in the inset panel (b). It can be clearly seen in Fig. 4 that single

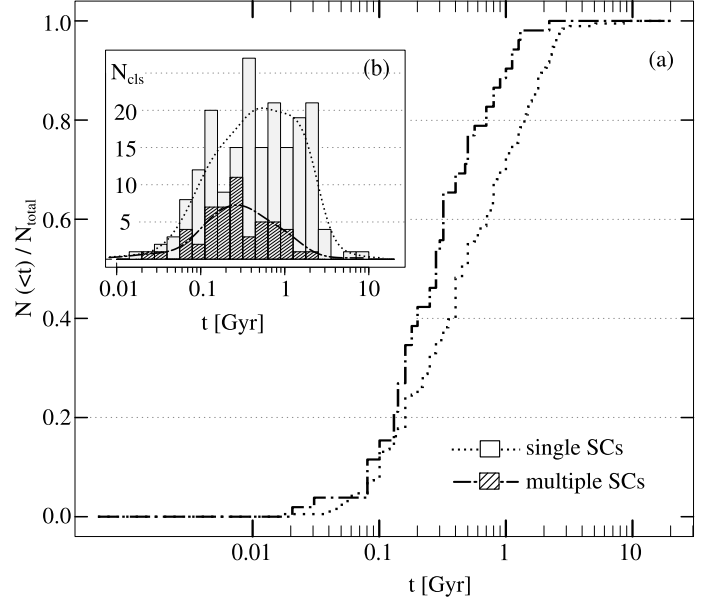


Fig. 4: Age distributions for multiple and single LMC clusters. The empirical cumulative distributions for multiple systems (dashed dotted line) and single SCs (dotted line) are shown. On the inset panel (b), the corresponding age histograms are shown (empty and shaded bars for single and multiple SCs, respectively) together with the kernel density estimations of both distributions (solid lines).

LMC SCs are typically older than multiple SCs. This difference is reflected both in the means and the shapes of the distributions. The Welch t-test (Welch 1947), designed to test if two samples have the same mean, is more reliable than the Student t-test applied when the two samples have different sizes and unknown variances which are suspected of being also different. We used the Student-test to measure the difference in the age values of single and multiple systems. We found that the statistic for the difference of the sample means belongs to the confidence interval (0.11, 0.37) to a statistical significance level of 95%. The mean age values are 0.48 and 0.27 Gyr for single and multiple star cluster samples, respectively. The F-test (Snedecor & Cochran 1989) is useful to determine if two populations have similar dispersions. The F-test uses the ratio of the sample variances as the test statistic, which follows an F distribution and thus permits testing the hypothesis that the ratio of the variances equals one. Although the variance for the sample of single SCs is approximately 40% larger than that of multiple SCs, the F statistic for the quotient of the variances is not conclusive when discarding the null hypothesis of the variances being equal ($v_1/v_2 = 1.43$, $p = 0.132$). Besides, both multiple and single SCs exhibit asymmetrical distributions in $\log(\text{age})$, the latter being slightly more asymmetric than that of the multiple SCs. This is quantified by the skewness values of -0.212 and -0.196 obtained for single and multiple SCs, respectively, meaning that the tail of older clusters appears to be flatter and falls more abruptly. In spite of the distribution shapes appearing wide, kurtosis values are 2.42 and 3.02 for simple and multiple SCs, respectively. These values indicate that the tails of the distributions are truncated with respect to a Gaussian distribution. The kernel density estimations of the two age distributions are also shown in panel (b) of Fig. 4. This does not depend on the bin size used to build the age histogram and contributes to enhance the distribution asymmetry, especially for single SCs.

5.2.4. Age determinations with different models

The ages resulting from isochrone fittings when different models of the Padova group are used will now be compared. We will call the ages estimated using Girardi et al. (2002) and Bressan et al. (2012) models t_G and t_B , respectively. In order to compare the resulting ages in these two cases, we show the relation existing between both age determinations in panels (a) and (b) of Fig. 5. In panels (c) and (d) of the same figure, the age ECDFs and the cumulative distributions of age determination uncertainties are respectively presented. As shown in the upper panel (a), if a logarithmic age relation is adopted, the differences between the resulting ages when one or the other set of isochrones is used are not very noticeable. A linear fit in panel (a) yields a slope $\alpha = 0.98$, slightly smaller than $\alpha = 1$, which would correspond to the absence of a systematic differences between the two models. However, differences in some objects arise when the ratio of age determinations is considered. Panel (b) exhibits the behaviour as a function of age of the ratio t_B/t_G between ages derived using these two models. Values of this ratio larger than 1 indicate that the cluster age determinations using Bressan et al. isochrones are larger than those using Girardi et al. isochrones. As can be seen in panel (b), t_G values have been generally underestimated compared to t_B values. In fact, only in 2.5% of the studied cluster sample can we find that $t_G > t_B$, which means that only 2 out of the 82 clusters of our sample fulfill this relation. 11 of the clusters have ages which are virtually identical whereas in the remaining 87% the relation $t_B > t_G$ holds. The excess in age, measured in Gyr, is at least 12% for 50 out of the 82 clusters of the sample S1 and even larger than 50% for the 5 clusters exhibiting the greatest differences. As shown in panel (c) of Fig. 5, the shapes of the two distributions in logarithmic scale are similar. The small shift between these two distributions accounts for the previously mentioned differences. It is seen in panel (d) that not only are t_B values typically larger than those of t_G but also that Bressan et al. age uncertainties are clearly smaller than the corresponding ones of Girardi et al. In panel (d), a KS-test yields $p = 0.125$ with t in Gyr units. For example, half of the age error values obtained using Girardi et al. isochrones are smaller than 0.04 Gyr, while the median of the error values obtained from Bressan et al. isochrones is nearly 0.03 Gyr. Even if the errors involved when ages are determined using one or the other set of isochrones are almost the same, the "more continuous" distribution of the Bressan et al. metallicities lead to more precise fittings and hence to more accurately determined cluster parameters. We would like to point out that while there are global differences in age determinations, when individual clusters are considered, the ages inferred from the two involved models turn out to be practically indistinguishable, as can be observed in Table 3.

Acknowledgements. We gratefully acknowledge financial support from the Argentinian institutions CONICET, FONCYT and SECYT (Universidad Nacional de Córdoba). Support for T.P. is provided by the Ministry of Economy, Development, and Tourism's Millennium Science Initiative through grant IC120009, awarded to The Millennium Institute of Astrophysics, MAS. D.G. gratefully acknowledges support from the Chilean BASAL Centro de Excelencia en Astrofísica y Tecnologías Afines (CATA) grant PFB-06/2007. This work is based on observations made at Cerro Tololo Inter-American Observatory, which is operated by AURA, Inc., under cooperative agreement with the National Science Foundation. Part of this work was supported by the German *Deutsche Forschungsgemeinschaft*, DFG project number Ts 17/2-1. We especially thank the referee for his valuable comments and suggestions about the manuscript. Plots were generated using R software and post-processed with Inkscape. This research has made use of NASA's Astrophysics Data System.

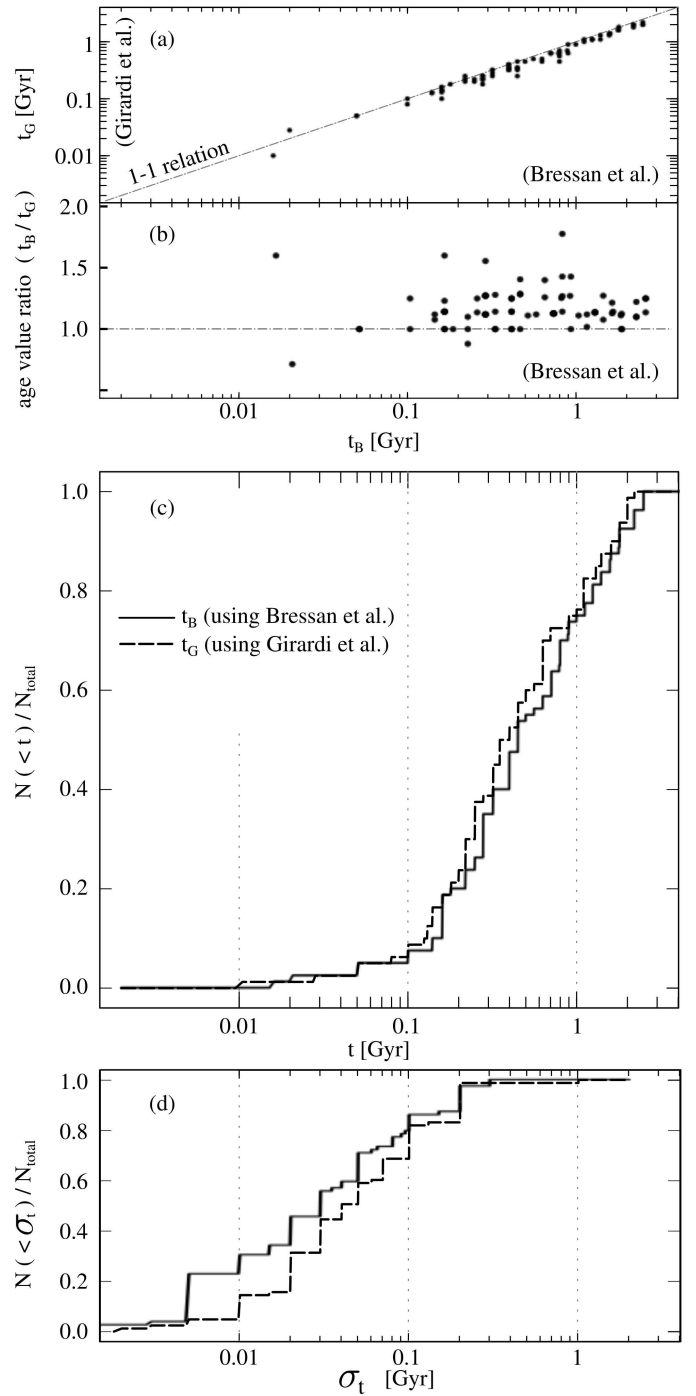


Fig. 5: Age determinations using Girardi et al. (2002) (dashed line) or Bressan et al. (2012) (solid line) set of isochrones. In the upper panel (a), the correlation between age estimates determined using both sets of isochrones is shown. A linear fit (not shown in the diagram) yields a slope of 0.98, which implies a slight bias towards greater age estimations when computed with Bressan et al.'s models. A 1-to-1 relation (dot dashed line) is also shown for the sake of comparison. In panel (b), the ratio between ages obtained using Bressan et al. and Girardi et al. models is presented. Values larger than 1 mean that Bressan et al. age estimates are larger. In panel (c), the age ECDFs using Bressan et al. isochrones (solid line) and Girardi et al. isochrones (dashed line) are plotted. The uncertainty distributions are represented by the corresponding cumulative distributions in the bottom panel (d).

References

- Bhatia, R. K., Read, M. A., Hatzidimitriou, D., & Tritton, S. 1991, A&AS, 87, 335
- Bica, E., Bonatto, C., Dutra, C. M., & Santos Jr., J. F. C. 2008, MNRAS, 389, 678
- Bica, E., Geisler, D., Dottori, H., et al. 1998, AJ, 116, 723
- Bica, E., Schmitt, H. R., Dutra, C. M., & Oliveira, H. L. 1999, AJ, 117, 238
- Bok, B. J. 1966, ARA&A, 4, 95
- Bothun, G. D. & Thompson, I. B. 1988, AJ, 96, 877
- Bressan, A., Marigo, P., Girardi, L., et al. 2012, MNRAS, 427, 127
- Burstein, D. & Heiles, C. 1982, AJ, 87, 1165
- Canterna, R. 1976, AJ, 81, 228
- Choudhury, S., Subramaniam, A., & Piatti, A. E. 2015, AJ, 149, 52
- Clariá, J. J., Piatti, A. E., Parisi, M. C., & Ahumada, A. V. 2007, MNRAS, 379, 159
- Clariá, J. J., Piatti, A. E., Santos, Jr., J. F. C., et al. 2005, Boletín de la Asociación Argentina de Astronomía, La Plata, Argentina, 48, 140
- Da Costa, G. S. & Armandroff, T. E. 1990, AJ, 100, 162
- Dieball, A., Müller, H., & Grebel, E. K. 2002, A&A, 391, 547
- Drion, E. F. 1952, Ann. Math. Statist., 23, 563
- Geisler, D. 1987, AJ, 93, 1081
- Geisler, D., Bica, E., Dottori, H., et al. 1997, AJ, 114, 1920
- Geisler, D., Clariá, J. J., & Minniti, D. 1991, AJ, 102, 1836
- Geisler, D., Piatti, A. E., Bica, E., & Clariá, J. J. 2003, MNRAS, 341, 771
- Geisler, D. & Sarajedini, A. 1999, AJ, 117, 308
- Girardi, L., Bertelli, G., Bressan, A., et al. 2002, A&A, 391, 195
- Glatt, K., Grebel, E. K., & Koch, A. 2010, A&A, 517, A50
- Harris, J. & Zaritsky, D. 2009, AJ, 138, 1243
- Hodge, P. W. 1975, Irish Astronomical Journal, 12, 77
- Hodge, P. W. 1988, PASP, 100, 1051
- Hodge, P. W. & Sexton, J. A. 1966, AJ, 71, 363
- Holtzman, J. A., Gallagher, III, J. S., Cole, A. A., et al. 1999, AJ, 118, 2262
- Kennicutt, Jr., R. C., Bresolin, F., Bomans, D. J., Bothun, G. D., & Thompson, I. B. 1995, AJ, 109, 594
- Kontizas, E., Metaxa, M., & Kontizas, M. 1988, AJ, 96, 1625
- Kontizas, M., Morgan, D. H., Hatzidimitriou, D., & Kontizas, E. 1990, A&AS, 84, 527
- Lejeune, T. & Schaerer, D. 2001, A&A, 366, 538
- Lyngå, G. & Westerlund, B. E. 1963, MNRAS, 127, 31
- Olsen, K. A. G. & Salyk, C. 2002, AJ, 124, 2045
- Olszewski, E. W., Harris, H. C., Schommer, R. A., & Canterna, R. W. 1988, AJ, 95, 84
- Palma, T., Clariá, J. J., Geisler, D., et al. 2011, BAAA, 54, 195
- Palma, T., Clariá, J. J., Geisler, D., Gramajo, L. V., & Ahumada, A. V. 2015, MNRAS, 450, 2122
- Palma, T., Clariá, J. J., Geisler, D., Piatti, A. E., & Ahumada, A. V. 2013, A&A, 555, A131
- Parker, J. W., Hill, J. K., Cornett, R. H., et al. 1998, AJ, 116, 180
- Piatti, A. E. 2011, MNRAS, 418, L40
- Piatti, A. E. 2012, A&A, 540, A58
- Piatti, A. E. 2014, MNRAS, 440, 3091
- Piatti, A. E. & Bica, E. 2012, MNRAS, 425, 3085
- Piatti, A. E., Bica, E., Geisler, D., & Clariá, J. J. 2003a, MNRAS, 344, 965
- Piatti, A. E., Clariá, J. J., Parisi, M. C., & Ahumada, A. V. 2009a, New A, 14, 97
- Piatti, A. E., Clariá, J. J., Parisi, M. C., & Ahumada, A. V. 2011, PASP, 123, 519
- Piatti, A. E., Geisler, D., Bica, E., & Clariá, J. J. 2003b, MNRAS, 343, 851
- Piatti, A. E., Geisler, D., Sarajedini, A., & Gallart, C. 2009b, A&A, 501, 585
- Piatti, A. E., Sarajedini, A., Geisler, D., Bica, E., & Clariá, J. J. 2002, MNRAS, 329, 556
- Pietrzyński, G. & Udalski, A. 2000, Acta Astron., 50, 337
- Pietrzyński, G., Udalski, A., Kubiak, M., et al. 1998, Acta Astronómica, 48, 175
- Pietrzyński, G., Udalski, A., Kubiak, M., et al. 1999, Acta Astronómica, 49, 521
- Popescu, B., Hanson, M. M., & Elmegreen, B. G. 2012, ApJ, 751, 122
- Press, W. H., Flannery, B. P., Teukolsky, S. A., & Vetterling, W. T. 1992, Numerical Recipes in Fortran 77: The Art of Scientific Computing, 2nd edition (Cambridge University Press)
- Ross, S. M. 2012, Simulation (Academic Press)
- Saha, A., Olszewski, E. W., Brondel, B., et al. 2010, AJ, 140, 1719
- Schlegel, D. J., Finkbeiner, D. P., & Davis, M. 1998, ApJ, 500, 525
- Shapley, H. & Lindsay, E. M. 1963, Irish Astronomical Journal, 6, 74
- Smecker-Hane, T. A., Cole, A. A., Gallagher, III, J. S., & Stetson, P. B. 2002, ApJ, 566, 239
- Snedecor, G. & Cochran, W. G. 1989, Statistical Methods (Iowa State University Press)
- Subramanian, S. & Subramanian, A. 2009, A&A, 496, 399
- Welch, B. L. 1947, Biometrika, 34, 28

Table 2: LMC star clusters observed in the Washington photometric system

Star Cluster ^a	α_{2000} (hms)	δ_{2000} (dms)	l (deg)	b (deg)	r ^b (arcmin)
HS 8,KMHK 5	04 30 40	-66 57 25	278.862	-38.343	0.40
SL 5,LW 8,KMHK 14	04 35 38	-73 43 54	286.402	-35.237	0.60
NGC 1644,SL 9,LW 11,ESO 84-30,KMHK 18	04 37 39	-66 11 58	277.649	-37.963	1.65
SL 8,LW 13,KMHK 21	04 37 52	-69 01 42	280.975	-36.949	0.75
SL 13,LW 17,KMHK 31	04 39 42	-74 01 02	286.573	-34.861	0.65
KMHK 58	04 43 14	-73 48 43	286.224	-34.721	0.43
KMHK 72	04 46 05	-66 54 41	278.156	-36.940	0.33
SL 33,LW 59,KMHK 91	04 46 25	-72 34 06	284.717	-34.986	0.55
SL 35,LW 58,KMHK 84	04 46 40	-67 41 07	279.052	-36.645	0.44
KMHK 95	04 47 26	-67 39 36	278.994	-36.584	0.23
SL 41,LW 64,KMHK 105	04 47 30	-72 35 18	284.704	-34.903	0.72
NGC 1697,SL 44,ESO 56-5,KMHK 110	04 48 37	-68 33 31	280.011	-36.196	1.15
KMHK 123	04 49 00	-72 38 24	284.713	-34.780	0.30
KMHK 112	04 49 07	-67 20 30	278.556	-36.528	0.50
KMHK 128	04 49 14	-72 03 24	285.177	-34.613	0.26
SL 48,LW 68,KMHK 133	04 49 27	-72 46 54	284.859	-34.698	0.45
LW 69,KMHK 137	04 49 41	-72 14 50	284.243	-34.873	0.28
KMHK 151	04 50 21	-72 49 36	284.881	-34.619	0.28
BSDL 77	04 50 29	-67 19 36	278.489	-36.407	0.30
SL 54,LW 78,KMHK 162	04 50 48	-72 34 36	284.582	-34.677	0.55
BSDL 87	04 50 58	-67 36 36	278.808	-36.279	0.25
HS 38,KMHK 148	04 51 11	-67 32 01	278.710	-36.282	0.35
HS 41,KMHK 158	04 51 30	-67 27 15	278.605	-36.276	0.29
KMHK 183	04 51 41	-72 13 13	284.147	-34.739	0.36
SL 73,LW 86,KMHK 214	04 52 45	-72 31 05	284.454	-34.561	0.34
SL 72,LW 87,KMHK 217	04 52 54	-72 10 23	284.055	-34.668	0.43
KMHK 229	04 53 52	-69 34 14	281.016	-35.435	0.40
BSDL 192	04 54 05	-69 40 54	281.138	-35.382	0.16
BSDL 194	04 54 05	-69 45 30	281.227	-35.359	0.21
NGC 1751,SL 89,ESO 56-23,KMHK 239	04 54 12	-69 48 25	281.280	-35.334	0.75
SL 96,H88-25,KMHK 256	04 55 01	-67 42 51	278.795	-35.880	0.41
H88-26	04 55 03	-67 57 52	279.089	-35.806	0.45
H88-32	04 55 39	-67 43 34	278.788	-35.819	0.21
H88-34,KMHK 285,MSX LMC 1238	04 55 39	-67 49 19	278.900	-35.793	0.29
KMHK 286	04 55 42	-67 46 54	278.851	-35.799	0.38
BSDL 268	04 55 52	-69 42 21	281.110	-35.227	0.26
BRHT 60b,H88-41,KMHK 309s	04 56 26	-67 56 19	279.013	-35.689	0.30
NGC 1764,SL 115,KMHK 308	04 56 28	-67 41 46	278.725	-35.754	0.55
H88-40,KMHK 310	04 56 29	-67 37 22	278.638	-35.772	0.38
SL 124w,KMHK 324w	04 56 29	-69 59 00	281.413	-35.094	0.29
SL 124e,KMHK 324e	04 56 32	-69 58 54	281.409	-35.090	0.29
KMHK 335	04 56 51	-70 06 03	281.537	-35.029	0.30
BRHT 45b	04 56 52	-68 00 20	279.079	-35.632	0.25
HS 72,BRHT 45a,KMHK 326	04 56 54	-68 00 08	279.073	-35.630	0.31
BSDL 320	04 57 08	-70 06 42	281.542	-35.002	0.20
SL 126,ESO 85-21,KMHK 322	04 57 22	-62 32 05	272.479	-36.910	0.65
SL 132,KMHK 348	04 57 26	-67 41 07	278.681	-35.668	0.50
SL 133,LW 99,KMHK 337	04 57 34	-65 16 00	275.788	-36.273	0.68
H88-52,KMHK 365	04 58 10	-68 03 37	279.102	-35.500	0.45
H88-55,KMHK 367	04 58 15	-67 46 02	278.753	-35.571	0.53
BSDL 341	04 58 15	-68 02 57	279.086	-35.495	0.28
SL 151,KMHK 388	04 58 51	-69 57 28	281.311	-34.908	0.63
H88-67	04 58 54	-67 50 49	278.827	-35.491	0.26
SL 154,H88-73,KMHK 390	04 59 15	-67 54 32	278.889	-35.442	0.60
NGC 1793,SL 163,ESO 56-43,KMHK 405	04 59 38	-69 33 22	280.816	-34.957	0.60
NGC 1795,SL 165,ESO 56-44,KMHK 411	04 59 46	-69 48 04	281.100	-34.876	0.68
SL 162,H88-79,KMHK 406	04 59 53	-67 55 25	278.888	-35.381	0.53
BRHT 62a,H88-84,KMHK 412	05 00 04	-67 48 02	278.737	-35.396	0.45
KMHK 506	05 04 29	-68 20 55	279.257	-34.859	0.34
BSDL 527	05 04 34	-68 12 30	279.088	-34.886	0.21

Table 2: continued.

Star Cluster ^a	α_{2000} (hms)	δ_{2000} (dms)	l (deg)	b (deg)	r ^b (arcmin)
SL 218, LOGLE 80	05 05 25	-68 30 04	279.411	-34.738	0.46
NGC 1836, SL 223, ESO 56-31, BRHT 4a	05 05 36	-68 37 46	279.557	-34.690	0.73
BRHT 4b, LOGLE 83	05 05 40	-68 38 12	279.563	-34.682	0.48
BSDL 594, LOGLE 87	05 05 54	-67 02 58	277.678	-35.038	0.43
NGC 1839, SL 226, ESO 56-63, LOGLE 93	05 06 03	-68 37 37	279.542	-34.650	0.80
HS 114, KMHK 533	05 06 02	-68 01 35	278.831	-34.798	0.43
NGC 1838, SL 225, ESO 56-64, LOGLE 97	05 06 09	-68 26 45	279.325	-34.686	0.63
HS 116, KMHK 536	05 06 13	-68 03 53	278.873	-34.772	0.26
SL 229, BRHT 29a, LOGLE 105	05 06 25	-68 22 22	279.231	-34.679	0.51
SL 230, BRHT 29b, OGLE 107	05 06 32	-68 21 44	279.216	-34.671	0.68
BSDL 631, LOGLE 109	05 06 34	-68 25 38	279.292	-34.653	0.23
H88-131, KMHK 544	05 06 41	-67 50 28	278.596	-34.781	0.35
LOGLE 122	05 07 19	-68 20 54	279.179	-34.605	0.12
BSDL 654, LOGLE 123	05 07 21	-66 49 45	277.377	-34.949	0.21
LOGLE 127	05 07 32	-67 34 13	278.253	-34.766	0.28
NGC 1846, SL 243, ESO 56-67, KMHK 557	05 07 35	-67 27 39	278.119	-34.786	1.9
SL 244	05 07 37	-68 32 31	279.399	-34.532	0.50
HS 121, KMHK 560	05 07 46	-67 51 41	278.590	-34.678	0.35
BSDL 665, LOGLE 130	05 07 47	-66 47 53	277.329	-34.914	0.21
BSDL 675, LOGLE 134	05 07 56	-67 21 28	277.990	-34.776	0.29
KMHK 575, LOGLE 139	05 08 28	-66 46 14	277.278	-34.854	0.47
KMHK 586	05 08 51	-67 58 49	278.704	-34.552	0.28
BSDL 716, GKK-O217	05 08 53	-68 05 01	278.825	-34.525	0.68
SL 263, LOGLE 144	05 08 54	-66 47 08	277.285	-34.809	0.24
GKK-O222	05 09 00	-67 59 00	278.704	-34.537	0.73
HS 131	05 09 12	-68 26 39	279.244	-34.414	0.20
HS 130, KMHK 588	05 09 15	-67 42 00	278.362	-34.577	0.28
SL 262, LW 146, ESO 119-40, KMHK 582	05 09 21	-62 22 46	271.976	-35.577	0.80
NGC 1852, SL 264, ESO 56-71, KMHK 594	05 09 23	-67 46 42	278.450	-34.547	0.95
BSDL 761	05 10 02	-66 42 00	277.155	-34.717	0.32
GKK-O220	05 10 18	-67 51 00	278.512	-34.447	0.78
HS 151	05 10 30	-68 24 02	279.161	-34.308	0.29
BSDL 779, LOGLE 182	05 10 32	-66 56 24	277.428	-34.619	0.22
SL 281, KMHK 616, LOGLE 183	05 10 33	-67 07 39	277.650	-34.579	0.62
SL 290, KMHK 628	05 10 36	-70 29 15	281.605	-33.806	0.53
BSDL 783, LOGLE 186	05 10 39	-66 43 45	277.174	-34.651	0.26
NGC 1860, SL 284, ESO 56-75, LOGLE 187	05 10 40	-68 45 13	279.570	-34.212	0.55
BSDL 794	05 10 46	-67 29 06	278.069	-34.483	0.19
H88-188, KMHK 622, LOGLE 191	05 10 54	-67 28 16	278.049	-34.474	0.30
HS 154, H88-189, KMHK 625, LOGLE 194	05 10 56	-67 37 36	278.233	-34.437	0.35
SL 293, KMHK 630	05 11 09	-67 40 57	278.295	-34.405	0.46
HS 156, H88-190, KMHK 632, LOGLE 199	05 11 11	-67 37 37	278.227	-34.414	0.25
NGC 1863, SL 299, ESO 56-77, LOGLE 206	05 11 40	-68 43 36	279.514	-34.131	0.65
SL 300, H88-198, KMHK 638, LOGLE 207	05 11 41	-67 33 56	278.142	-34.381	0.46
NGC 1865, SL 307, ESO 56-78, LOGLE 221	05 12 25	-68 46 19	279.549	-34.055	0.70
SL 310, KMHK 652, LOGLE 224	05 12 30	-67 17 28	277.797	-34.359	0.43
NGC 1864, SL 309, ESO 56-79	05 12 40	-67 37 24	278.187	-34.276	0.51
BSDL 923	05 13 43	-67 24 10	277.901	-34.223	0.23
HS 178, KMHK 667	05 13 48	-66 37 12	276.970	-34.367	0.34
NGC 1885, SL 338, ESO 56-88, LOGLE 261	05 15 07	-68 58 43	279.729	-33.772	0.65
BSDL 1024, LOGLE 262	05 15 15	-68 52 57	279.614	-33.782	0.41
LOGLE 264	05 15 21	-69 06 27	279.875	-33.725	0.18
H88-232	05 15 22	-69 02 32	279.798	-33.737	0.23
BSDL 1035	05 15 25	-68 40 52	279.373	-33.808	0.23
HS 198	05 15 26	-69 03 02	279.807	-33.730	0.26
HS 200, LOGLE 269	05 15 36	-69 08 21	279.907	-33.697	0.43
LOGLE 271	05 15 39	-68 54 31	279.635	-33.741	0.45
H88-238, LOGLE 276	05 15 47	-69 14 39	280.027	-33.659	0.38
H88-240, LOGLE 282	05 16 04	-69 06 09	279.853	-33.664	0.33
H88-245, LOGLE 288	05 16 27	-69 04 49	279.819	-33.635	0.26

Table 2: continued.

Star Cluster ^a	α_{2000} (hms)	δ_{2000} (dms)	l (deg)	b (deg)	r^b (arcmin)
H88-249	05 16 31	-69 10 58	279.939	-33.608	0.23
HS 205,LOGLE 290	05 16 32	-68 55 07	279.627	-33.660	0.55
H88-252	05 16 43	-69 12 13	279.958	-33.586	0.39
H88-253,LOGLE 296	05 16 50	-69 03 35	279.786	-33.605	0.38
LOGLE 297	05 16 52	-69 04 13	279.798	-33.600	0.12
SL 351	05 16 56	-68 40 58	279.341	-33.673	0.38
H88-259,LOGLE 306	05 17 20	-69 09 25	279.890	-33.542	0.51
H88-260,LOGLE 307	05 17 20	-69 12 49	279.956	-33.530	0.36
H88-261,LOGLE 310	05 17 26	-69 06 55	279.838	-33.542	0.51
SL 359,KMHK 727	05 17 49	-68 28 22	279.075	-33.635	0.60
H88-265,LOGLE 323	05 18 05	-69 10 18	279.891	-33.474	0.29
H88-269,LOGLE 337	05 18 41	-69 04 46	279.770	-33.439	0.33
LOGLE 340	05 18 47	-69 13 32	279.939	-33.402	0.32
H88-270	05 18 47	-69 16 37	279.999	-33.392	0.23
NGC 1917,SL 379,ESO 56-100,LOGLE 343	05 19 02	-69 00 04	279.671	-33.422	0.85
H88-272	05 19 05	-68 52 14	279.515	-33.445	0.26
OGLE 346	05 19 09	-69 15 36	279.972	-33.363	0.22
HS 228	05 19 24	-68 52 52	279.522	-33.415	0.30
SL 390,LOGLE 356	05 19 54	-68 57 53	279.609	-33.354	0.55
H88-276	05 19 55	-68 48 07	279.418	-33.384	0.26
LOGLE 363	05 20 04	-69 15 55	279.959	-33.282	0.15
SL 388,LW 186,ESO 85-72,KMHK 773	05 20 05	-63 28 49	273.090	-34.211	0.85
SL 397	05 20 12	-68 54 15	279.534	-33.341	0.50
H88-281	05 20 21	-69 14 48	279.932	-33.262	0.29
H88-285	05 21 03	-69 05 51	279.741	-33.229	0.38
SL 408A	05 21 05	-69 04 16	278.896	-34.889	0.41
H88-286	05 21 07	-69 08 09	279.787	-33.216	0.20
H88-287	05 21 09	-69 07 02	279.763	-33.216	0.24
BSDL 1334, 88-259 ,LOGLE 306	05 21 14	-68 47 00	279.369	-33.271	0.23
HS 247	05 21 45	-68 55 02	279.516	-33.201	0.38
BSDL 1364	05 21 46	-68 43 53	279.298	-33.233	0.21
HS 253,LOGLE 403	05 22 03	-70 02 44	280.833	-32.962	0.29
KMK88-52	05 22 17	-70 02 00	280.814	-32.945	0.25
IC 2134,SL 437,LW 198,ESO 33-19,KMHK 864	05 23 06	-75 26 48	287.049	-31.698	0.70
HS 264,KMHK 845	05 23 12	-70 46 40	281.666	-32.725	0.40
SL 451,LW 206,KMHK 883	05 24 13	-75 34 00	287.166	-31.600	0.50
SL 446A,KMHK 858	05 24 28	-67 43 43	278.067	-33.156	0.46
SL 444,KMHK 861	05 24 30	-67 40 41	278.006	-33.161	0.54
LW 211,KMHK 901	05 25 27	-73 34 13	284.858	-31.979	0.33
SL 460,LOGLE 456	05 25 28	-69 46 32	280.453	-32.724	0.38
SL 469,LOGLE 467	05 25 57	-69 45 04	280.415	-32.687	0.43
KMHK 907	05 26 12	-70 58 53	281.847	-32.445	0.26
BSDL 1723,LOGLE 473	05 26 24	-69 43 51	280.384	-32.652	0.33
NGC 1969,SL 479,ESO 56-124	05 26 34	-69 50 27	280.509	-32.619	0.60
NGC 1971,SL 481,ESO 56-128	05 26 46	-69 51 03	280.518	-32.601	0.51
NGC 1972,SL 480,ESO 56-129	05 26 49	-69 50 17	280.502	-32.599	0.42
KMK88-57,LOGLE 483	05 26 53	-69 48 54	280.473	-32.596	0.29
SL 490,LW 217,KMHK 939	05 27 18	-73 40 48	284.951	-31.828	0.58
H 14,SL 506,LW 220,KMHK 967	05 28 39	-73 37 49	284.871	-31.745	0.70
SL 505,KMHK 960	05 28 50	-71 37 58	282.560	-32.120	0.58
SL 510,KMHK 968	05 29 20	-70 34 46	281.325	-32.262	0.36
KMHK 979,GKK-O101	05 29 39	-70 59 02	281.790	-32.168	0.30
HS 329,KMHK 984	05 29 46	-71 00 02	281.807	-32.156	0.35
SL 509,LW 221,ESO 85-91,KMHK 957	05 29 48	-63 38 58	273.152	-33.118	0.93
LW 224	05 29 56	-72 03 17	283.030	-31.959	0.21
KMHK 975	05 29 59	-67 52 44	278.151	-32.618	0.19
LW 231,KMHK 1031	05 30 26	-75 20 57	286.813	-31.270	0.45
LW 231,KMHK 1031	05 30 26	-75 20 54	286.813	-31.270	0.45
NGC 1997,SL 520,LW 226,ESO 86-1,KMHK 978	05 30 34	-63 12 12	272.612	-33.071	0.90
KMHK 993	05 30 34	-68 09 27	278.469	-32.526	0.28

Table 2: continued.

Star Cluster ^a	α_{2000} (hms)	δ_{2000} (dms)	l (deg)	b (deg)	r ^b (arcmin)
SL 548,LW 235,KMHK 1035	05 31 24	-72 02 33	282.990	-31.848	0.33
SL 555,LW 236,KMHK 1046	05 31 42	-72 08 46	283.108	-31.805	0.70
KMHK 1023	05 31 46	-68 14 08	278.544	-32.405	0.31
SL 551,RHT 38a,KMHK1027,GKK-O202	05 31 51	-67 59 28	278.255	-32.429	0.49
KMHK 1029	05 31 57	-67 52 43	278.122	-32.435	0.31
BRHT 38b,KMHK 1032	05 31 58	-67 58 18	278.228	-32.420	0.35
SL549,KMHK1013	05 32 03	-64 14 32	273.828	-32.819	0.70
KMHK 1045	05 32 23	-67 59 49	278.255	-32.379	0.30
KMHK 1055	05 33 02	-67 50 56	278.072	-32.337	0.40
H 3,SL 569,KMHK 1065	05 33 20	-68 09 08	278.424	-32.272	0.90
IC 2140,SL 581,LW 241,ESO 33-24,KMHK 1106	05 33 21	-75 22 35	286.800	-31.084	1.15
SL 579,KMHK 1085	05 34 13	-67 51 23	278.066	-32.224	0.48
SL 588,KMHK 1101	05 34 39	-68 18 20	278.587	-32.129	0.68
IC 2146,SL 632,LW 258,ESO 33-26,KMHK 1178	05 37 46	-74 46 58	286.058	-30.917	1.65
LW 263,KMHK 1208	05 39 08	-74 51 12	286.120	-30.817	0.48
H88-306	05 40 24	-69 15 10	279.623	-31.505	0.28
H88-313	05 41 21	-69 03 46	279.391	-31.441	0.20
HS 390,MHK1239	05 41 30	-69 11 06	279.532	-31.416	0.33
H88-315,GKK-O164	05 41 38	-69 18 48	279.680	-31.391	0.25
NGC 2093,SL 657,ESO 56-23	05 41 49	-68 55 15	279.221	-31.414	0.70
H88-320,MHK 1248	05 41 58	-69 02 51	279.365	-31.388	0.30
H88-321	05 42 08	-69 22 00	279.737	-31.341	0.19
SL 663,LW 273,ESO 86-22,KMHK 1250	05 42 29	-65 21 46	275.053	-31.629	0.95
H88-325	05 43 15	-69 02 03	279.337	-31.275	0.23
SL 674,ESO 86-26,KMHK 1281	05 43 20	-66 15 44	276.100	-31.487	0.80
H88-326	05 43 29	-69 09 44	279.484	-31.242	0.24
SL 678,KMHK1283	05 43 35	-66 12 31	276.034	-31.464	0.58
H88-327,KMHK1295	05 43 38	-69 15 51	279.603	-31.219	0.35
H88-329,KMHK1297	05 43 43	-69 13 23	279.554	-31.216	0.29
NGC 2108,SL 686,ESO 57-33,KMHK 1304	05 43 56	-69 10 50	279.503	-31.200	0.90
H88-331,MHK1313	05 44 11	-69 20 00	279.677	-31.165	0.31
SL 691,BRHT 40a,KMHK 1319	05 44 14	-70 39 20	281.213	-31.027	0.38
SL 692,BRHT 40b,KMHK 1320	05 44 15	-70 40 10	281.229	-31.025	0.48
BSDL 2938,LOGLE 717	05 44 42	-70 25 31	280.941	-31.013	0.23
HS 406,KMHK 1332,LOGLE 720	05 44 47	-70 24 22	280.917	-31.008	0.33
HS 409,KMHK 1336,LOGLE 721	05 44 57	-70 19 59	280.831	-31.001	0.28
BSDL 2950,LOGLE 723	05 45 01	-70 32 34	281.074	-30.974	0.23
BSDL 2963,LOGLE 727	05 45 20	-70 36 06	281.139	-30.941	0.23
SL 704,KMHK 1343,LOGLE 728	05 45 25	-70 24 05	280.905	-30.955	0.39
H88-333	05 45 27	-69 20 43	279.679	-31.052	0.26
HS 410,KMHK 1344,LOGLE 729	05 45 32	-70 45 34	281.320	-30.910	0.36
BSDL 2972,LOGLE 731	05 45 46	-70 43 09	281.271	-30.894	0.24
HS411,MHK1345	05 45 50	-69 22 49	279.716	-31.016	0.23
HS412,MHK1347	05 45 56	-69 16 19	279.589	-31.016	0.35
BSDL 2978,LOGLE 732	05 45 59	-70 43 46	281.281	-30.876	0.20
LOGLE 733	05 46 11	-70 43 12	281.268	-30.860	0.17
SL 707,KMHK 1353	05 46 12	-69 04 57	279.366	-31.008	0.65
BSDL 2993,LOGLE 735	05 46 37	-70 46 33	281.329	-30.820	0.24
HS 414,BRHT 42b,KMHK 1365	05 46 41	-70 50 52	281.411	-30.807	0.44
SL 716,BRHT 42a,KMHK 1367	05 46 47	-70 49 58	281.393	-30.800	0.53
BSDL 3001,LOGLE 738	05 46 48	-70 35 21	281.111	-30.823	0.40
BSDL 2995	05 46 51	-69 25 11	279.754	-30.923	0.23
BSDL 3000,LOGLE 739	05 46 51	-70 30 40	281.019	-30.825	0.24
BSDL 3003,LOGLE 740	05 46 52	-70 48 21	281.361	-30.796	0.23
H88-334,KMHK 1363	05 46 52	-69 11 23	279.486	-30.940	0.36
BSDL 3050	05 48 00	-70 28 30	280.968	-30.734	0.34
KMHK 1389	05 48 12	-70 28 00	280.956	-30.718	0.38
BSDL 3060	05 48 12	-70 33 24	281.061	-30.710	0.37
HS 420,KMHK 1403	05 48 28	-70 32 52	281.049	-30.688	0.34
BSDL 3072	05 48 33	-70 29 00	280.973	-30.687	0.40

Table 2: continued.

Star Cluster ^a	α_{2000} (hms)	δ_{2000} (dms)	l (deg)	b (deg)	r ^b (arcmin)
BSDL 3071	05 48 35	-70 18 39	280.773	-30.699	0.20
KMHK 1408	05 48 46	-70 28 23	280.959	-30.670	0.55
SL 736	05 49 17	-70 47 54	281.331	-30.599	0.36
HS 424,KMHK 1425	05 49 36	-70 41 35	281.207	-30.582	0.39
H 7,SL 735,ESO 57-43,BM 109	05 50 03	-67 43 05	277.753	-30.746	1.15
SL 748,KMHK 1437	05 50 15	-70 25 40	280.895	-30.550	0.60
HS 427,KMHK 1443	05 50 17	-70 36 56	281.111	-30.532	0.43
KMHK 1448	05 50 28	-70 32 33	281.027	-30.523	0.34
BSDL 3123	05 50 45	-70 34 34	281.063	-30.497	0.23
C 11	05 50 48	-71 42 28	282.371	-30.397	0.20
BSDL 3158	05 52 11	-71 51 30	282.533	-30.276	0.46
KMHK 1504	05 53 15	-71 53 32	282.563	-30.191	0.32
SL 769,KMHK 1499	05 53 23	-70 04 16	280.459	-30.310	0.90
H88-365,KMHK 1507	05 53 27	-71 41 10	282.325	-30.192	0.34
SL 775,LW 327,KMHK 1506	05 53 27	-71 42 57	282.359	-30.189	0.60
OHSC 28	05 55 35	-62 20 43	271.508	-30.237	0.35
NGC 2161,SL 789,LW 337,ESO 33-31,KMHK 1544	05 55 42	-74 21 14	285.376	-29.793	1.15
NGC 2153,SL 792,LW 341,ESO 86-43,KMHK 1555	05 57 51	-66 24 02	276.200	-30.025	0.75
NGC 2155,SL 803,LW 347,ESO 86-45,KMHK 1563	05 58 33	-65 28 37	275.134	-29.958	1.20
SL 817,KMHK 1588	06 00 38	-70 04 10	280.425	-29.695	0.70
SL 826,LW 363,KMHK,1606	06 01 52	-72 21 19	283.046	-29.500	0.75
ESO 121-03,KMHK 1591	06 02 02	-60 31 24	269.451	-29.382	1.05
LW 393,KMHK 1648	06 06 31	-72 13 35	282.882	-29.151	0.26
LW 397,KMHK 1657	06 07 29	-72 29 39	283.187	-29.071	0.34
SL 842,LW 399,ESO 86-61,KMHK 1652	06 08 15	-62 59 15	272.323	-28.814	0.85
KMHK 1668	06 08 53	-72 23 02	283.056	-28.968	0.29
NGC 2213,SL 857,LW 419,ESO 57-70,KMHK 1681	06 10 42	71 31 44	282.078	-28.839	1.05
SL 862,LW 431,ESO 57-75,KMHK 1692	06 13 27	-70 41 45	281.128	-28.613	0.85
SL 870,LW 440,KMHK 1705	06 14 28	-72 36 34	283.310	-28.546	0.58
SL 869,LW 341,KMHK 1704	06 14 41	-69 48 07	280.114	-28.490	0.80
KMHK 1702	06 14 54	-72 30 19	283.190	-28.586	0.31
OHSC 33,KMHK 1714	06 15 17	-73 47 07	284.647	-28.482	0.20
SL 874,LW 446,ESO 57-77,KMHK 1713	06 15 57	-70 04 23	280.426	-28.390	0.75
KMHK 1719	06 17 19	-70 03 39	280.417	-28.273	0.44
LW 469,KMHK 1742	06 21 34	-72 47 24	283.522	-28.021	0.53
SL 896,LW 480,KMHK 1758	06 29 58	-69 20 01	279.677	-27.131	0.50
OHSC 37,KMHK 1762	07 07 39	-69 59 02	280.983	-24.011	0.29

Notes. (a) Cluster identifications from (SL): Shapley & Lindsay (1963); (LW): Lyngå & Westerlund (1963); (HS): Hodge & Sexton (1966); (C): Hodge (1975); H88: Hodge (1988); (OHSC): Olszewski et al. (1988); (KMK): Kontizas et al. (1988); (KMHK): Kontizas et al. (1990); (BRHT): Bhatia et al. (1991); (LOGLE): Pietrzyński et al. (1998, 1999); (BSDL): Bica et al. (1999). (b) Obtained from Bica et al. (2008)

Table 3: Fundamental parameters for the star cluster sample

ID	Radius (arcmin)	Deproj. dist (deg)	$E(B - V)$	Age _I (Gyr)	[Fe/H] _I (dex)	Age _{II} (± 0.30 Gyr)	[Fe/H] _{II} (± 0.3 dex)	Notes	Ref
HS 8	...	6.2	0.026	1.60	1
SL 5	...	6.8	0.082	2.50	1
NGC 1644	...	6.3	0.018	2.50	1
SL 8	...	4.2	0.040	1.60 / 1.80	-0.50	a	2,3
SL 13	...	6.8	0.049	2.50	1
KMHK 58	...	6.5	0.089	1.60	1
LW 54	0.30	5.0	0.000	0.40 ± 0.08	-0.40	a	4
SL 33	0.90	5.1	0.116	$2.20^{+0.3}_{-0.2}$	-0.40	...	-0.60	m1	5,17
SL 35	...	4.3	0.051	1.50	...	a	1
KMHK 95	0.35	4.2	0.041	0.35 ± 0.07	-0.40	4
SL 41	0.99	5.1	0.116	1.58 ± 0.20	-0.57	1.40	5,17
NGC 1697	1.67	3.5	0.040	0.70 ± 0.10	0.00	6
KMHK 123	0.50	5.0	0.118	1.12 ± 0.10	-0.54	5,17
KMHK 112	...	4.4	0.048	1.25	...	a	1
KMHK 128	0.50	5.4	0.111	1.60 ± 0.20	-0.84	...	-0.90	...	5,17
SL 48	0.90	5.1	0.118	2.50 ± 0.30	-0.72	2.10	-0.80	...	7
LW 69	0.54	4.6	0.122	1.80 ± 0.20	-0.72	1.70	5,17
KMHK 151	0.77	5.1	0.118	1.40 ± 0.20	-0.72	1.40	-0.80	...	5,17
BSDL 77	0.40	4.3	0.000	0.79 ± 0.16	-0.40	4
SL 54	0.90	4.9	0.120	1.00 ± 0.10	-0.47	5,17
BSDL 87	0.18	4.0	0.050	0.08 ± 0.01	-0.40	b	8
HS 38	0.25	4.0	0.050	0.40 ± 0.10	-0.40	a,b	9
HS 41	0.18	4.1	0.048	0.06 ± 0.01	-0.40	a	8
KMHK 183	0.72	4.5	0.122	0.79 ± 0.09	-0.40	a	9
SL 73	0.86	4.7	0.120	1.78 ± 0.20	-0.70	1.60	-0.80	...	5,17
SL 72	0.72	4.4	0.133	0.28 ± 0.03	-0.40	5,17
KMHK 229	0.25	2.6	0.100	1.00 ± 0.20	-0.40	a,b	9
BSDL 192	0.18	2.6	0.102	0.10 ± 0.01	-0.40	m2 / a,b	8
BSDL 194	0.14	2.6	0.102	0.25 ± 0.03	-0.40	b	8
NGC 1751	...	2.6	0.102	1.30	1
SL 96	...	3.6	0.058	1.60	1
H88-26	0.33	3.3	0.060	0.80 ± 0.20	-0.40	b	9
H88-32	0.14	3.5	0.058	0.25 ± 0.03	-0.40	b	8
H88-34	0.14	3.1	0.058	0.25 ± 0.03	-0.40	b	8
H88-33	0.30	3.4	0.066	$0.16-0.32 \pm 0.20$	-0.40	b	4
BSDL 268	0.99	2.5	0.102	0.09 ± 0.02	-0.40	a,b	4
BRHT 60b	0.14	3.2	0.060	0.08 ± 0.01	-0.40	m3 / a,b	8
NGC 1764	0.23	3.5	0.058	0.08 ± 0.01	-0.40	a,b	8
H88-40	0.33	3.5	0.060	0.70 ± 0.20	-0.40	b	9
SL 124w	0.14	2.5	0.115	0.50 ± 0.05	-0.40	m4	8
SL 124e	0.14	2.5	0.115	0.50 ± 0.05	-0.40	m4 / b	8
KMHK 335	0.09	2.5	0.115	0.10 ± 0.01	-0.40	b	8
BRHT 45b	0.14	3.2	0.060	0.08 ± 0.01	-0.40	m5 / a,b	8
BRHT 45a	0.45	3.2	0.076	0.13 ± 0.03	-0.40	m5 / a,b	4
BSDL 320	0.14	2.5	0.115	0.10 ± 0.01	-0.40	a,b	8
SL 126	...	8.9	0.000	2.50 / 2.20	-0.45	...	2,3
SL 132	...	3.4	0.057	1.60	...	a	1
SL 133	1.13	5.9	0.020	2.00 ± 0.20	-0.70	2.30	6
H88-52	0.45	3.0	0.041	1.12 ± 0.23	-0.40	1.40	...	m6 / b	1,4
H88-55	0.33	3.3	0.060	0.50 ± 0.10	-0.40	b	9
BSDL 341	0.40	3.0	0.086	0.28 ± 0.06	-0.40	m6 / b	4
SL 151	...	2.3	0.102	1.50	1
H88-67	...	3.1	0.062	1.70	1
SL 154	0.33	3.0	0.060	0.50 ± 0.10	-0.40	b	9
NGC 1793	0.42	2.1	0.107	0.11 ± 0.02	-0.40	a,b	4
NGC 1795	...	2.1	0.096	1.60	1
SL 162	...	3.0	0.062	1.50	...	a	1
BRHT 62a	0.32	3.1	0.062	0.16 ± 0.02	-0.40	a,b	8
KMHK 506	0.17	2.2	0.060	0.56 ± 0.07	-0.40	9
BSDL 527	...	2.4	0.059	1.40	1

Table 3: continued.

ID	Radius (arcmin)	Deproj. dist (deg)	$E(B - V)$	Age _I (Gyr)	[Fe/H] _I (dex)	Age _{II} (± 0.30 Gyr)	[Fe/H] _{II} (± 0.3 dex)	Notes	Ref
SL 218	...	2.0	0.060	0.05 ± 0.01	-0.40	a,b,c	10
NGC 1836	...	1.9	0.060	0.40 ± 0.10	0.00	m7 / b	11
BRHT 4b	...	1.9	0.060	0.10 ± 0.02	-0.40	m7 / a,c	10
BSDL 594	0.63	3.4	0.046	$1.58^{+0.20}_{-0.17}$	-0.47	1.30	...	c	5,17
HS 113	0.23	2.2	0.059	0.20 ± 0.02	-0.40	m8	8
NGC 1839	...	1.9	0.060	0.13 ± 0.02	-0.40	a,b	10
HS 114	...	2.4	0.055	1.30	1
NGC 1838	...	2.0	0.060	0.10 ± 0.02	-0.40	a	10
HS 116	0.30	2.4	0.041	0.35 ± 0.07	-0.40	4
SL 229	0.33	2.1	0.060	0.32 ± 0.10	-0.40	...	-0.40	m9 / c	4,9
SL 230	0.42	2.1	0.081	0.08 ± 0.02	-0.40	m9 / a	4
BSDL 631	0.25	2.0	0.000	0.22 ± 0.05	-0.40	a,c	4
H88-131	0.40	2.6	0.030	1.00 ± 0.21	-0.40	4
OGLE 122	0.18	2.0	0.059	0.40 ± 0.04	-0.40	c	8
BSDL 654	0.34	3.6	0.033	0.22 ± 0.03	-0.02	c	5,17
LOGLE 127	0.23	2.8	0.061	0.10 ± 0.01	-0.40	c	8
NGC 1846	...	2.9	0.061	1.40	1
SL 244	...	1.8	0.060	1.60 / 1.30	-0.30	b	2,12
HS 121	...	2.5	0.060	1.50	1
BDSL 665	0.27	3.6	0.033	0.90 ± 0.10	-0.41	c	5,17
BSDL 675	0.41	3.0	0.061	1.40 ± 0.20	-0.40	1.40	...	c	5,17
KMHK 575	0.59	4.2	0.043	$0.89^{+0.23}_{-0.19}$	c	7
KMHK 586	...	2.3	0.055	1.80	1
BSDL 716	0.50	2.2	0.060	0.40 ± 0.10	-0.40	9
SL 263	0.45	3.6	0.043	$0.02^{+0.006}_{-0.005}$	-0.23	c	7
GKK-O222	0.14	2.3	0.055	1.58 ± 0.16	-0.40	8
HS 131	0.45	1.8	0.081	1.26 ± 0.26	-0.40	4
HS 130	0.41	2.5	0.061	0.16 ± 0.02	-0.41	5,17
SL 262	...	8.6	0.001	2.10	-0.55	...	2,3
NGC 1852	...	2.5	0.060	1.40	1
BSDL 761	0.41	3.6	0.036	0.16 ± 0.02	-0.40	5,17
GKK-O220	0.23	2.3	0.060	0.79 ± 0.08	-0.40	8
HS 151	0.33	1.8	0.060	0.79 ± 0.10	-0.40	9
BSDL 779	0.36	3.3	0.043	0.10 ± 0.01	-0.02	c	5,17
SL 281	0.95	3.1	0.052	$0.05^{+0.006}_{-0.005}$	-0.31	a,c	17
SL 290	...	1.7	0.101	1.20	...	a	1
BSDL 783	0.32	3.6	0.072	0.16 ± 0.01	-0.30	a,c	17
NGC 1860	...	1.4	0.080	0.25 ± 0.50	0.00	b,c	11
BSDL 794	0.45	2.7	0.060	$0.80^{+0.3}_{-0.17}$	-0.41	m10	7
H88-188	0.41	2.7	0.061	$0.63^{+0.08}_{-0.07}$	-0.27	m10 / c	9,17
HS 154	0.33	2.5	0.060	$0.45-0.50 \pm 0.10$	-0.40	m11 / c	4,9
SL 293	0.63/0.5	2.5	0.061	0.40 ± 0.05	-0.31	9,17
HS 156	0.54	2.5	0.061	$1.25^{+0.2}_{-0.1}$	$0.40^{+0.47}_{-0.47}$	m11 / c	4,5,8,17
NGC 1863	...	1.4	0.060	0.04 ± 0.01	-0.40	a,b,c	10
SL 300	0.67	2.6	0.060	0.40 ± 0.10	-0.40	c	9
NGC 1865	...	1.3	0.060	0.50 ± 0.10	-0.20	m12 / c	2,11
SL 310	0.68	2.8	0.061	0.05 ± 0.01	-0.30	a,c	17
NGC 1864	0.99	2.5	0.061	0.25 ± 0.03	-0.40	a	17
BSDL 923	0.41	2.7	0.060	$0.10^{+0.02}_{-0.01}$	-0.36	a	17
HS 178	0.54	3.5	0.036	0.71 ± 0.08	-0.41	5
NGC 1885	0.32	0.9	0.081	0.06 ± 0.01	-0.40	c	8
BSDL 1024	1.00	1.0	0.080	0.16 ± 0.03	-0.40	c	9
OGLE 264	0.18	0.7	0.078	0.63 ± 0.06	-0.40	c	8
H88-232	0.18	0.8	0.078	0.13 ± 0.01	-0.40	m13 / c	8
BSDL 1035	0.17	1.2	0.060	0.50 ± 0.10	-0.40	9
HS 198	0.14	0.8	0.078	0.14 ± 0.01	-0.40	m13 / b,c	8
HS 200	0.18	0.7	0.086	0.50 ± 0.05	-0.40	b,c	8
OGLE 271	0.27	0.9	0.078	0.40 ± 0.04	-0.40	c	8
H88-238	0.23	0.6	0.090	0.13 ± 0.01	-0.40	b,c	8

Table 3: continued.

ID	Radius (arcmin)	Deproj. dist (deg)	$E(B - V)$	Age _I (Gyr)	[Fe/H] _I (dex)	Age _{II} (± 0.30 Gyr)	[Fe/H] _{II} (± 0.3 dex)	Notes	Ref
H88-240	0.27	0.7	0.081	0.20 ± 0.02	-0.40	b,c	8
H88-245	0.50	0.7	0.080	0.16 ± 0.04	-0.40	b,c	9
H88-249	0.14	0.6	0.090	0.32 ± 0.03	-0.40	8
HS 205	0.27	0.8	0.081	0.10 ± 0.01	-0.40	c	8
H88-252	0.23	0.6	0.090	0.25 ± 0.03	-0.40	b	8
H88-253	0.18	0.7	0.081	0.20 ± 0.02	-0.40	m14 / c	8
OGLE 297	0.27	0.7	0.081	0.08 ± 0.01	-0.40	b,c	8
SL 351	0.33	1.1	0.060	0.50 ± 0.10	-0.40	9
H88-259	0.18	0.6	0.081	0.79 ± 0.08	-0.40	c	8
H88-260	0.18	0.5	0.090	0.40 ± 0.04	-0.40	c	8
H88-261	0.32	0.6	0.081	0.50 ± 0.05	-0.40	c	8
SL 359	...	1.3	0.060	1.60	-0.4	...	2,12
H88-265	0.33	0.5	0.051	0.20 ± 0.04	-0.40	b,c	4
H88-269	0.33	0.5	0.051	0.79 ± 0.16	-0.40	c	4
OGLE 340	0.36	0.4	0.090	0.04 ± 0.00	-0.40	c	8
H88-270	0.18	0.3	0.090	1.26 ± 0.13	-0.40	b	8
NGC 1917	...	0.6	0.081	1.30	1
H88-272	0.23	0.8	0.060	0.32 ± 0.03	-0.40	m15	8
OGLE 346	0.25	0.3	0.090	0.16 ± 0.02	-0.40	c	8
HS 228	0.27	0.7	0.060	1.26 ± 0.13	-0.40	m15 / b	8
SL 390	0.32	0.6	0.081	1.00 ± 0.10	-0.40	b,c	8
H88-276	0.23	0.8	0.060	0.79 ± 0.08	-0.40	b	8
OGLE 363	0.18	0.3	0.090	0.10 ± 0.01	-0.40	c	8
SL 388	0.50	7.0	0.030	2.2 / 2.6	-0.65	...	2,3
SL 397	0.42	0.7	0.081	0.16 ± 0.03	-0.40	a,b	4
H88-281	0.23	0.3	0.090	0.16 ± 0.02	-0.40	b	8
H88-285	0.18	0.4	0.081	0.32 ± 0.03	-0.40	m16 / b	8
SL 408A	0.23	0.5	0.055	0.14 ± 0.01	-0.40	a,b	8
H88-286	0.14	0.4	0.081	0.32 ± 0.03	-0.40	m16 / a	8
H88-287	0.23	0.4	0.081	0.16 ± 0.02	-0.40	m16 / b	8
BSDL 1334	0.18	0.8	0.060	1.00 ± 0.10	-0.40	b,c	8
HS 247	0.33	0.6	0.127	0.35 ± 0.07	-0.40	b	4
BSDL 1364	0.09	0.9	0.060	0.16 ± 0.02	-0.40	8
HS 253	0.45	0.7	0.085	$0.22^{+0.03}_{-0.02}$	-0.36	b,c	17
KMK88-52	0.45	0.6	0.085	0.18 ± 0.02	+0.02	m17	17
IC 2134	0.50	6.9	0.107	1.00	3
HS 264	...	1.5	0.083	1.60	...	a	1
SL 451	...	7.0	0.106	2.20	-0.70	...	2,3
SL 446A	...	2.0	0.060	2.20 ± 0.50	-0.90	2.30 / 2.40	-0.75	a	2,12
SL 444	...	2.0	0.060	0.50 ± 0.10	-0.40	a	11
LW 211	0.72	4.7	0.097	$1.80^{+0.4}_{-0.2}$	-0.67	5,17
SL 460	0.72	0.5	0.062	$0.02^{+0.012}_{-0.006}$	-0.47	m18 / c	17
SL 469	0.54	0.5	0.062	0.16 ± 0.02	-0.44	c	17
KMHK 907	0.35	1.7	0.091	0.25 ± 0.05	-0.40	4
BSDL 1723	0.45	0.5	0.062	0.28 ± 0.03	-0.40	c	17
NGC 1969	0.63	0.5	0.062	$0.16^{+0.09}_{-0.03}$	-0.54	m19	17
NGC 1971	0.50	0.5	0.062	$0.14^{+0.11}_{-0.3}$	-0.47	m19	17
NGC 1972	0.36	0.5	0.062	$0.16^{+0.09}_{-0.03}$	-0.44	m19	17
KMK88-57	0.41	0.6	0.062	$0.80^{+0.2}_{-0.24}$	-0.54	m20 / c	17
SL 490	0.99	4.8	0.120	$2.20^{+0.30}_{-0.40}$	-0.66	1.80	-0.80	...	7,13
SL 506	1.35	4.8	0.106	1.80 ± 0.20	-0.66	1.70	-0.80	...	17
SL 505	...	2.5	0.070	0.90 ± 0.20	-0.50	1.60 / 1.50	-0.70	a	2,12
SL 510	0.17	1.4	0.080	0.13 ± 0.03	-0.40	a	9
KMHK 979	0.33	1.8	0.086	0.08 ± 0.02	-0.40	m21 a	4
HS 329	0.65	1.8	0.000	$0.79-1.00 \pm 0.23$	-0.40	1.80	...	m21	1,6
SL 509	...	6.6	0.030	1.40 / 1.20	-0.85	...	2,3
LW 224	...	3.0	0.060	0.70 ± 0.10	0.00	m22	11
KMHK 975	0.35	1.9	0.051	0.20 ± 0.04	-0.40	4
LW 231	0.52	6.7	0.110	$0.80^{+0.20}_{-0.17}$	-0.50	7,13

Table 3: continued.

ID	Radius (arcmin)	Deproj. dist (deg)	$E(B - V)$	Age _I (Gyr)	[Fe/H] _I (dex)	Age _{II} (± 0.30 Gyr)	[Fe/H] _{II} (± 0.3 dex)	Notes	Ref
NGC 1997	0.80	7.1	0.040	2.60 \pm 0.50	-0.70	2.70	6
KMHK 993	0.18	1.6	0.062	0.10 \pm 0.01	-0.40	8
SL 548	...	3.0	0.080	0.40 \pm 0.10	0.00	11
SL 555	...	3.1	0.070	1.60 \pm 0.30	-0.70	1.60 / 1.80	-0.75	a	2,12
KMHK 1023	...	1.6	0.062	1.70	1
SL 551	0.33	1.8	0.091	0.14 \pm 0.03	-0.40	m23 / a,b	4
KMHK 1029	0.27	2.0	0.058	0.10 \pm 0.01	-0.40	b	8
BRHT 38b	0.50	1.9	0.081	0.18 \pm 0.04	-0.40	m23 / b	4
SL 549	...	5.9	0.040	2.00 \pm 0.50	-0.90	1.30 / 2.00	2,12
KMHK 1045	0.17	1.9	0.060	0.60 \pm 0.10	-0.40	b	9
KMHK 1055	0.17	2.0	0.060	1.00 \pm 0.20	-0.40	a,b	9
H 3	...	1.8	0.062	2.50	1
IC 2140	1.17	6.8	0.111	2.50 $^{+0.6}_{-0.5}$	-0.84	2.10	-1.10	...	7
SL 579	0.30	2.1	0.066	0.14 \pm 0.03	-0.40	a,b	4
SL 588	0.67	1.7	0.060	0.40 \pm 0.10	-0.40	b	9
IC 2146	...	6.1	0.117	1.60	1
LW 263	...	6.2	0.117	1.80	1
H88-306	0.14	1.8	0.063	0.13 \pm 0.01	-0.40	m24	8
H88-313	0.18	1.9	0.064	0.13 \pm 0.01	-0.40	b	8
HS 390	0.33	1.9	0.228	0.18 \pm 0.04	-0.40	b	4
H88-315	0.18	2.0	0.063	0.08 \pm 0.01	-0.40	a,b	8
NGC 2093	0.50	2.0	0.070	0.25 \pm 0.05	-0.40	m25 / a,b	9
H88-320	0.45	2.0	0.168	0.16 \pm 0.03	-0.40	a,b	4
H88-321	0.18	2.0	0.063	0.08 \pm 0.01	-0.40	b	8
SL 663	1.93	4.8	0.040	2.80 \pm 0.35	-0.70	3.30	6
H88-325	0.18	2.1	0.072	0.22 \pm 0.02	-0.40	8
SL 674	...	3.9	0.050	2.00 \pm 0.40	-0.90	2.10 / 2.30	-0.80	a	2,12
H88-326	0.18	2.1	0.072	0.32 \pm 0.03	-0.40	a,b	8
SL 678	...	4.0	0.050	1.50 \pm 0.30	-0.80	2.00	-0.80	a	12
H88-327	0.27	2.1	0.074	0.03 \pm 0.00	-0.40	m26	8
H88-329	0.18	2.2	0.072	0.06 \pm 0.01	-0.40	b	8
NGC 2108	...	2.2	0.072	1.25	1
H88-331	0.40	2.2	0.117	0.50 \pm 0.10	-0.40	4
SL 691	0.38	2.3	0.068	0.28 $^{+0.07}_{-0.08}$	-0.47	m27 / a,c	17
SL 692	0.47	2.3	0.068	0.25 \pm 0.03	-0.41	m27 / a,c	17
BSDL 2938	0.45	2.3	0.067	0.45 $^{+0.18}_{-0.10}$	-0.23	17
HS 406	0.32	2.3	0.067	0.32 $^{+0.03}_{-0.04}$	-0.23	c	17
HS 409	0.50	2.3	0.067	0.45 $^{+0.11}_{-0.13}$	-0.27	c	7
BSDL 2950	0.27	2.3	0.067	0.71 \pm 0.08	-0.36	c	17
BSDL 2963	0.52	2.4	0.068	1.25 $^{+0.2}_{-0.1}$	0.00	c	17
SL 704	0.45	2.3	0.067	0.45 $^{+0.11}_{-0.05}$	-0.16	c	17
H88-333	0.33	2.3	0.070	0.40 \pm 0.10	-0.40	9
HS 410	0.63	2.5	0.068	0.56 \pm 0.06	-0.27	c	17
BSDL 2972	0.43	2.5	0.068	0.71 $^{+0.09}_{-0.1}$	0.00	c	17
HS 411	0.25	2.4	0.173	0.28 \pm 0.06	-0.40	4
HS 412	0.42	2.4	0.173	0.13 \pm 0.03	-0.40	a	4
BSDL 2978	0.27	2.5	0.068	0.90 $^{+0.2}_{-0.27}$	-0.23	c	17
LOGLE 733	0.27	2.5	0.068	0.80 $^{+0.2}_{-0.24}$	-0.10	c	17
SL 707	...	2.4	0.072	2.30	1
BSDL 2993	0.59	2.5	0.068	0.71 \pm 0.08	-0.36	c	17
HS 414	0.45	2.6	0.086	0.32 $^{+0.03}_{-0.04}$	-0.31	m28 / a,c	17
SL 716	0.20	2.6	0.068	0.28 $^{+0.04}_{-0.03}$	-0.10	m28 / a,c	17
BSDL 3001	0.77	2.5	0.068	0.28 $^{+0.04}_{-0.03}$	-0.31	a,c	17
BSDL 2995	0.50	2.4	0.070	1.00 \pm 0.20	-0.40	m29	9
BSDL 3000	0.63	2.5	0.067	0.22 $^{+0.02}_{-0.03}$	0.00	c	17
BSDL 3003	0.41	2.6	0.068	0.45 \pm 0.05	-0.31	c	17
H88-334	...	2.5	0.072	2.00	1
BSDL 3050	0.34	2.5	0.067	0.28 $^{+0.04}_{-0.03}$	-0.31	m30	17
KMHK 1389	0.36	2.6	0.067	0.16 \pm 0.02	-0.31	m30	17

Table 3: continued.

ID	Radius (arcmin)	Deproj. dist (deg)	$E(B - V)$	Age _I (Gyr)	[Fe/H] _I (dex)	Age _{II} (± 0.30 Gyr)	[Fe/H] _{II} (± 0.3 dex)	Notes	Ref
BSDL 3060	0.50	2.6	0.067	$0.45^{+0.11}_{-0.1}$	-0.47	7
HS 420	0.41	2.6	0.073	$0.32^{+0.08}_{-0.07}$	-0.27	7
BSDL 3072	0.41	2.6	0.073	$0.40^{+0.16}_{-0.08}$	-0.31	m30	7
BSDL 3071	0.27	2.5	0.075	0.14 ± 0.20	-0.41	17
KMHK 1408	0.59	2.6	0.073	$0.50^{+0.13}_{-0.1}$	-0.33	m30	7
SL 736	0.90	2.7	0.070	$0.40^{+0.10}_{-0.08}$	-0.19	7
HS 424	0.50	2.7	0.074	$0.40^{+0.1}_{-0.08}$	-0.23	7
H7	...	3.2	0.065	1.40	2
SL 748	0.90	2.7	0.073	$0.25^{+0.07}_{-0.04}$	-0.36	m31 / a	17
HS 427	0.86	2.8	0.074	0.32 ± 0.03	-0.36	17
KMHK 1448	0.54	2.8	0.073	$0.28^{+0.04}_{-0.03}$	-0.31	17
BSDL 3123	0.32	2.8	0.073	$0.40^{+0.10}_{-0.08}$	-0.31	7
C11	0.68	3.4	0.101	0.40 ± 0.05	-0.31	5
BSDL 3158	0.99	3.5	0.101	2.50 ± 0.30	-0.40	2.10	-0.80	...	5,17
KMHK 1504	0.63	3.6	0.117	$2.20^{+0.30}_{-0.40}$	-0.72	...	-0.80	...	7
SL 769	0.076	1.80	-0.50	...	3
H88-365	0.41	3.5	0.101	0.28 ± 0.06	-0.40	a	13,17
SL 775	0.95	3.5	0.090	$0.63^{+0.17}_{-0.13}$	-0.50	7
OHSC 28	0.33	8.3	0.040	2.20 ± 0.25	-0.70	2.70	6
NGC 2161	1.50	5.9	0.130	1.10 ± 0.30	-0.70	14
NGC 2153	...	4.6	0.035	1.30	...	a	2
NGC 2155	...	5.4	0.050	3.20 ± 0.60	-0.90	3.60	15
SL 817	...	3.6	0.070	2.5 / 1.5	-0.50	...	2,3
SL 826	1.17	4.4	0.112	$2.50^{+0.70}_{-0.30}$	-0.78	2.10	-0.90	...	17
ESO 121-03	...	10.4	0.030	8.50	-1.05	...	2,3
LW 393	...	4.6	0.116	1.80	1
LW 397	...	4.9	0.109	1.80	1
SL 842	0.40	8.1	0.030	1.90 / 2.20	-0.60	...	2,3
KMHK 1668	...	4.9	0.109	1.70	1
NGC 2213	...	4.6	0.116	1.5	-0.40	16
SL 862	...	4.7	0.090	1.80	-0.85	...	2,3
SL 870	1.04	5.4	0.088	$1.25^{+0.2}_{-0.1}$	-0.40	1.20	5,17
SL 869	...	4.9	0.101	1.70	1
KMHK 1702	0.45	5.3	0.110	1.12 ± 0.10	-0.72	1.20	5,17
OHSC 33	...	6.2	0.090	1.20 / 1.40	-1.00	m32 / c	2,3
SL 874	0.84	4.9	0.090	1.50 ± 0.30	-0.70	14
KMHK 1719	0.42	5.1	0.090	1.40 ± 0.30	-0.60	14
LW 469	0.50	5.9	0.080	0.60 ± 0.10	-0.40	9
SL 896	...	6.4	0.070	2.30 ± 0.30	-0.60	2.30	15
OHSC 37	...	9.4	0.150	2.70 / 2.10	-0.65	...	2,3

Notes. Parameters obtained also by (a) Glatt et al. (2010), (b) Popescu et al. (2012), and (c) Pietrzyński & Udalski (2000)

The letter m indicates that the cluster belongs to a binary or multiple system.

References. 1) Piatti (2011); 2) Geisler et al. (1997); 3) Bica et al. (1998); 4) Choudhury et al. (2015); 5) Palma et al. (2013) ; 6) Piatti et al. (2009b); 7) Palma et al. (2015); 8) Piatti (2014); 9) Piatti (2012); 10) Piatti et al. (2003b); 11) Piatti et al. (2003a); 12) Geisler et al. (2003); 13) Palma et al. (2011); 14) Piatti et al. (2011); 15) Piatti et al. (2002); 16) Geisler (1987); 17) Present work